DRUG ENCAPSULATED POLYMERIC NANOPARTICLES FOR TARGETING CANCER CELLS

by

Sesil Genç

B.S., Molecular Biology and Genetics, Boğaziçi University, 2013

Submitted to the Institute for Graduate Studies in
Science and Engineeering in partial fulfillment of
the requirements for the degree of
Master of Science

Graduate Program in Chemistry

Boğaziçi University

2015

DRUG ENCAPSULATED POLYMERIC NANOPARTICLES FOR TARGETING CANCER CELLS

APPROVED BY:

Assoc. Prof. Rana Sanyal ……...
(Thesis Supervisor)

Assoc. Prof. Amitav Sanyal ……..

Asst. Prof. Ibrahim Yaman …….

DATE OF APPROVAL:…….

Dedicated to my family...

ACKNOWLEDGEMENTS

First I would wish to express my sincere gratitude to my thesis supervisor Assoc. Prof. Rana Sanyal and Assoc. Prof. Amitav Sanyal for their scientific guidence and support which enabled me to do this work. I have gained a great deal of knowledge about chemistry and experience in chemistry laboratory and learned how to cope with problems concerning research, from them. I really appreciate their endless attention and encouragement.

I would wish to thank to Assist. Prof. Ibrahim Yaman for his careful and constructive review of the final manuscript of the thesis.

I am so much thankful to Burcu Sümer Bolu for her generous help during my research besides her smart conversation and enjoyful friendship. I am also so much thankful to Özgül Gök for her very kind interest and endless help during my research. I am also thankful to Özlem for polymer synthesis and her helps in several areas of my research. I also thank to my labmates Harun, Hazal, Filiz, Laura, Ahmet, Aslı, Tuğçe, Yavuz, Sadık, Yasemin, Evrim, Duygu, Nergiz, Merve, Hasan Can, Mehmet, Sadık, Büşra, Buğra, Azize, Gizem and İsmail for sharing the joy of making research and their friendship. Especially I would wish to thank my friend Janset for her intimate friendship and support in every part of my life. I would also like to thank all present and previous group members and all the members of the faculty in my department.

My deepest thanks go to my family for their endless support during all of my education.

I am thankful to The Scientific and Technological Research Council of Turkey (TÜBİTAK) (BİDEB – 2211-D) for supporting this project.

ABSTRACT

DRUG ENCAPSULATED POLYMERIC NANOPARTICLES FOR TARGETING CANCER CELLS

Targeted drug delivery systems have gained much attention in recent years due to the fact that it offers useful solutions to the problems concerning chemotherapy drugs. The main aim in targeted drug delivery is to transport the chemotherapy agent directly to the cancer tissue without having side effects on the healthy tissues, with the help of nanocarriers. Also the bioavailability of the drugs are increased with nanocarriers. Polymeric nanoparticles are one of these nanocarriers. The reasons to choose polymeric nanoparticles among other nanocarriers are that they are easily produced, provide high drug encapsulation efficiency and stable enough to investigate their effects *in vitro*. In this study, first generation nanoparticles were prepared with PLA as a building block. Anticancer drug doxorubicin was physically loaded into hydrophobic core of the nanoparticles. To increase the drug loading efficiency, the drug molecules were conjugated to polymer chains of the nanoparticle by means of Diels-Alder reaction. To achieve this, furan-bearing PLA-carbonate copolymer was synhesized via ring opening polymerization, as a building block of the nanoparticles, whereas the drug molecules were modified with maleimide linker, EMCH. To enhance drug release profiles of the nanoparticles, mono-maleimide PEG chains were synthesized to conjugate to them via Diels-Alder reaction and second generation nanoparticles were produced. Finally, cRGDfK-maleimide molecules were attached to the PEG-PLA nanoparticles for active targeting also with Diels-Alder reaction and third generation nanoparticles were generated.

ÖZET

İLAÇ TAŞIYAN POLİMERİK NANOPARÇACIKLARIN KANSER HÜCRELERİNE HEDEFLENMESİ

Hedefleyici ilaç taşıyıma sistemleri kemoterapi ilaçları ile ilgili problemlere kullanışlı çözümler sunduğu için son yıllarda oldukça ilgi çekmektedir. Hedefleyici ilaç taşımadaki temel amaç, nanotaşıyıcılar yardımıyla kemoterapi ajanını sağlıklı dokular üzerine yan etkisi olmaksızın doğrudan kanser dokusuna taşımaktır. Nanotaşıyıcılar ayrıca ilaçların biyoyararlanımlarını artırmaktadır. Bu nanotaşıyıcılardan biri de polimerik nanoparçacıklardır. Nanotaşıyıcılar arasından polimerik nanoparçacıkların seçimesinin sebepleri kolay üretiliyor olmaları, yüksek ilaç kapsülleme verimi sağlamaları ve *in vitro* etkileri üzerine çalışılmasına yetecek kadar dayanıklı olmalarıdır. Bu çalışmada birinci jenerasyon nanoparçacıklar yapıtaşı olarak PLA kullanılarak hazırlandı. Antikanser ilacı doksorubisin nanoparçacıkların hidrofobik merkezine fiziksel olarak yüklendi. İlaç yükleme verimini artırmak için, ilaç molekülleri naanoparçacıkların polimer zincirlerine Diels-Alder reaksiyonu ile bağlandı. Bunu gerçekleştirmek için furan taşıyan PLA-karbonat kopolimeri nanoparçacıkların yapıtaşı olmak üzere halka açılımı polimerizasyonu ile sentezlendi, ayrıca ilaç molekülleri maleimid bağlayıcısıyla, EMCH, modifiye edildi. Nanoparçacıkların ilaç salınım profillerini geliştirmek için, onlara Diels-Alder reaksiyonu ile konjuge edilmek üzere mono-maleimid PEG zincirleri sentezlendi ve ikinci jenerasyon nanoparçacıklar oluşturuldu. Son olarak, PEG-PLA nanoparçacıklarına aktif hedefleme için yine Diels-Alder reaksiyonu ile cRGDfK-maleimid molekülleri bağlandı ve üçüncü jenerasyon nanoparçacıklar üretildi.

TABLE OF CONTENTS

LIST OF FIGURES

LIST OF TABLES

LIST OF ACRONYMS/ABBREVIATIONS

J	Coupling constant
$CDCl_3$	Deuterated chloroform
CH_2Cl_2	Dichloromethane
DA	Diels-Alder
DBU	1,8-Diazabicyclo[5.4.0]undec-7-ene
DCNP	Drug Conjugated Nanoparticle
DENP	Drug Encapsulated Nanoparticle
DLS	Dynamic Light Scatter
DMAP	4-Dimethylaminopyridine
DNA	Deoxyribo Nucleic Acid
Dox	Doxorubicin
EDCI	1-Ethyl-3-(3-dimethylaminopropyl)carbodiimide
EPR	Enhanced Permeability and Retention
EMCH	N-ε-maleimidocaproic
FT-IR	Fourier Transform Infrared
GPC	Gel Permeation Chromotography
MeOH	Methanol
$NaHCO_3$	Sodium Bicarbonate
Na_2SO_4	Sodium Sulphate
N_2	Nitrogen
NMR	Nuclear Magnetic Resonance
NP	Nanoparticle
P	Polymer
PDI	Polydispersity Index
PEG	Polyethylene Glycole
PLA	Polylactic acid
rDA	Retro Diels-Alder

RT	Room Temperature
TEA	Triethylamine
THF	Tetrahydrofuran
TU	1-(3,5-bis(trifluoromethyl)phenyl)-3-cyclohexyl-thiourea
UV	Ultraviolet

1. INTRODUCTION

1.1. Cancer and Chemotherapy

Cancer has been one of the most terminal diseases for years. According to World Health Organization (WHO), 8.2 million people died due to different types of cancer only in 2012 and only 30% of cancers can be prevented (Table 1.1)[1].

Table 1.1. All Cancers (excluding non-melanoma skin cancer) Estimated Incidence, Mortality and Prevalence Worldwide in 2012 [1].

Estimated numbers (thousands)	Cases	Deaths	5-year prev.
World	14068	8202	32455
More developed regions	6054	2878	16823
Less developed regions	8014	5323	15632
WHO Africa region (AFRO)	645	456	1363
WHO Americas region (PAHO)	2882	1295	7958
WHO East Mediterranean region (EMRO)	555	367	1194
WHO Europe region (EURO)	3715	1933	9701
WHO South-East Asia region (SEARO)	1724	1171	3278
WHO Western Pacific region (WPRO)	4543	2978	8956
IARC membership (24 countries)	7038	3470	18595
United States of America	1604	617	4775
China	3065	2206	5045
India	1015	683	1790
European Union (EU-28)	2635	1276	7157

In a healthy individual, when cells grow old or become damaged they undergo apoptosis, a type of programmed cell death. When cancer develops, this process breaks down. As time passes, the cells become more and more abnormal due to accumulation of mutations in the DNA. The telomere regions found at the ends of chromosomes do not shorten as the cell divides, which is shorten in a healthy cell in each division. By this way these cells become immortal and continuously divide and some of them form tumors and some of them spread into other tissues through the blood or the lymph system, which is called malignancy. A schematic representation of uncontrolled growth of cancer cells can be seen in Figure 1.1.

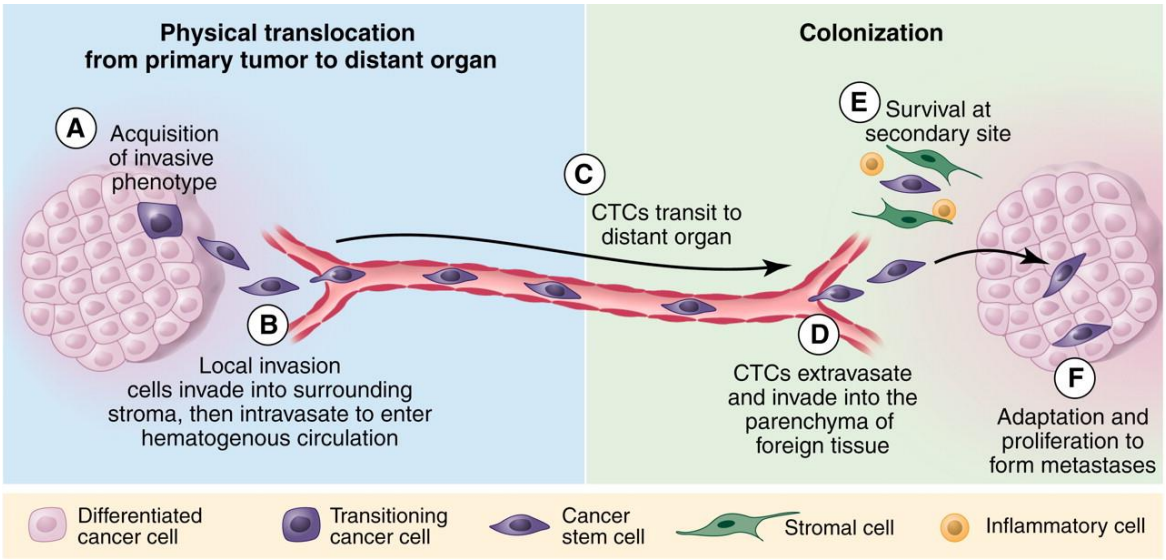

Figure 1.1. Loss of normal growth control [2].

There are many kinds of anticancer drugs according to their mechanism of action. Anthracyclines are one group of them. Their chemical structures can be seen in Figure 1.2. They are derived from *Streptomyces*. Dox has a broad spectrum of activity. It is one of the most effective drugs in treatment of solid tumors like breast cancer, small cell lung cancer and ovarian carcinoma treatments. It has important activity against bladder, liver, stomach and thyroid tumors, osteogenic bone tumors, soft tissue sarcoma, neuroblastoma, Wilms tumor, multiple myeloma, several types of leukemia and cutaneous T-cell lymphoma. It also plays a significant role in treatment of Hodgkins disease and non-Hodgkins lymphomas. Dox was shown to target the topoisomerase-II which has a key role in DNA replication and by this way prevents cellular replication [3].

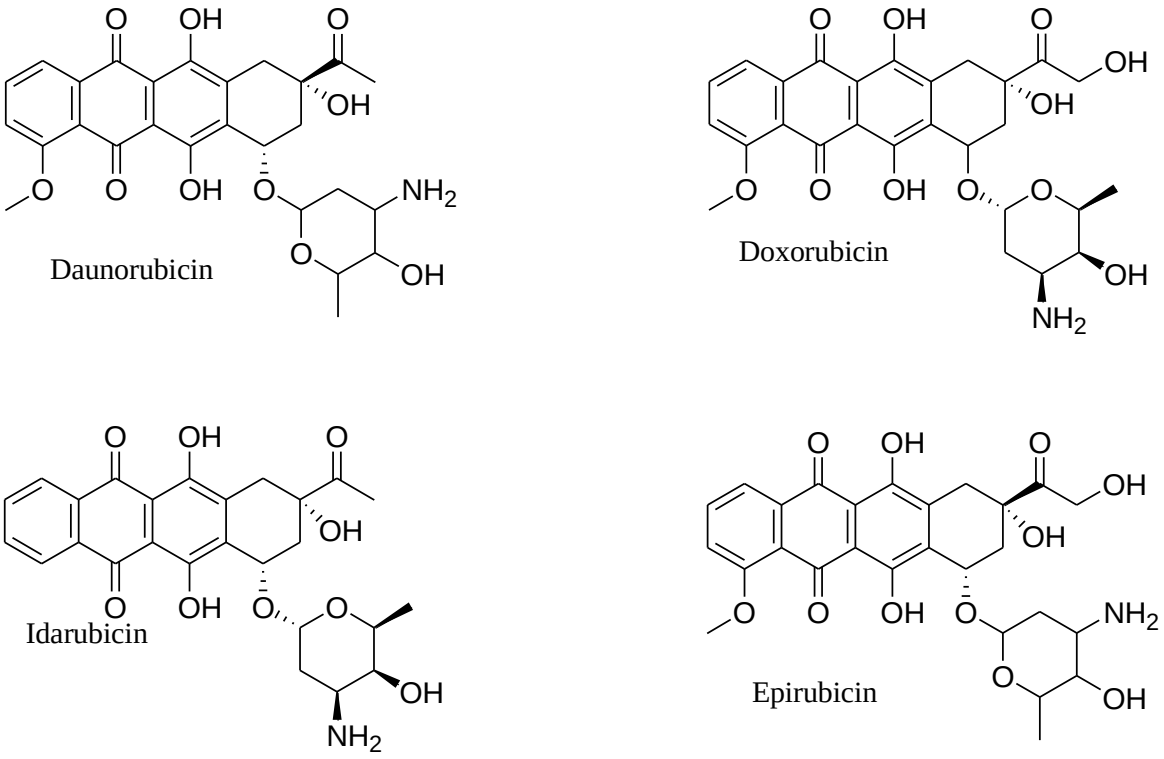

Figure 1.2. Structures of commonly used anthracyclins.

New studies are being conducted on nanometer or micrometer-sized nanocarriers which carry the anticancer drug specifically to cancer tissue with different mechanisms. Targeted drug delivery is one of the main mechanisms used in delivery of these nanocarriers to the cancerous tissue.

1.2. Targeted Drug Delivery

Chemotherapy and radiotherapy are the basic treatments for cancer patients. However, chemotherapeutic agents used in cancer treatment are toxic for healthy tissues as well as the cancerous tissues. The main reason for this cytotoxicity is that these drugs cannot discriminate healthy and cancerous cells. They have also dose-related systematic toxicity like gastrointestinal disorders, cardiotoxicity and extravasation [4]. Another problem with chemotherapy drugs is that most of them cause *myelosuppression*, a condition showing a decrease in the amount of bone marrow cells. These cells have a main role in production of

white blood cells which function as the defense mechanism of the whole organism. This is the reason why chemotherapy agents weaken the immune system of the patient. Also, most of the anticancer drugs have the common hydrophobicity issue, which causes low solubility of the agent in blood. On the other hand, the hydrophilic ones have short circulation time and rapid renal clearance. Therefore, they cannot be efficient enough in destroying cancer cells [5].

Targeted drug delivery aims to control the bioavailability and biodistribution profile of the drug in the patients' body. For this reason, selectivity of the drug bearing nanocarriers towards the targeted cell type and a better pharmacokinetic profile should be provided. These enhancements are obtained by passive and active tumor targeting [6].

1.2.1. Passive Tumor Targeting

In healthy tissues, there are capillaries which have a key role in feeding the cells in terms of glucose, oxygen, etc. In tumor tissues, the number of these capillaries is very high and the cells composing the walls of the capillaries are not well-ordered as the capillaries of the healthy tissues (Figure 1.3). The leaky structure of these capillary walls in tumor tissues cause bigger molecules to get into the tumor tissue. Also dysfunctional lymphatic drainage results in the retention of extravasated nanocarriers within tumor tissues. This situation is called as "enhanced permeability and retention" (EPR) effect. In order to target the tumor tissues, nanocarriers are designed to get inside the tumor through enlarged pores on the capillaries [7-8].

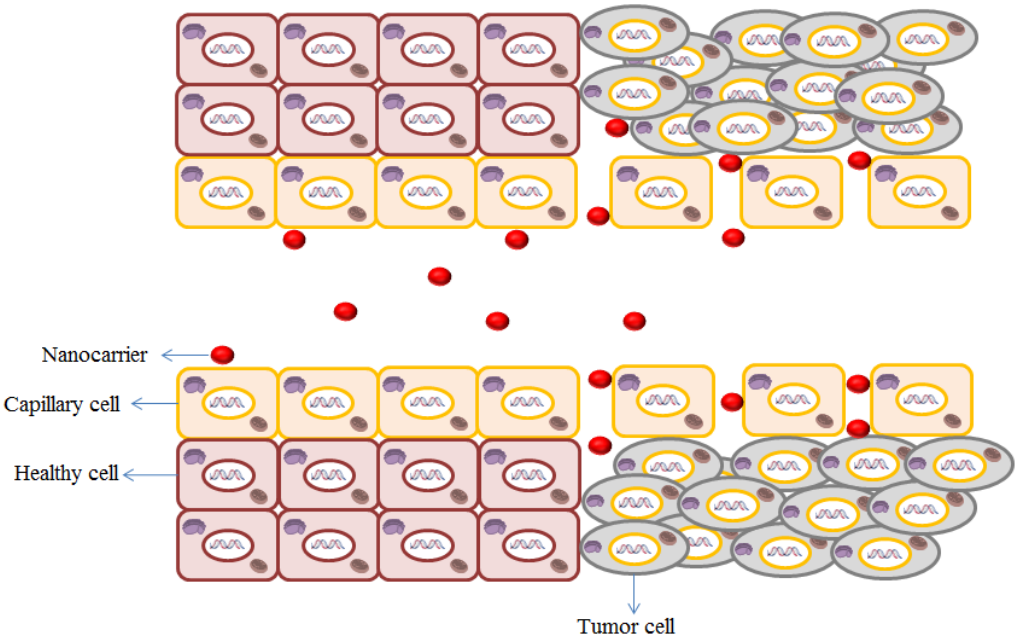

Figure 1.3. Enhanced permeation and retention effect.

Nanocarriers are designed in a way that they are big enough to accumulate in tumor tissue via EPR effect but cannot pass through the capillaries of the healthy tissues. Thus, drug molecules which are bound to or encapsulated by the nanocarriers are said to be "passively targeting" the tumor tissue. By this way drug accumulates in the tumor for a longer time, which is enough to kill the cancer cells. Nanocarriers have a variety of sizes changing between 10-500 nm in diameter [9].

1.2.2. Active Tumor Targeting

The cancer cells have many abnormalities compared to healthy cells. Expression of some receptors on cell membrane in excessive amounts is one of these abnormalities. If these receptors are targeted by drug carrying nanostructures, the probability of selection of a cancer cell rather than a healthy cell is much higher. So this mechanism is very useful to transport the cancer drug directly to the cancer cells as seen in schematic representation in Figure 1.4.

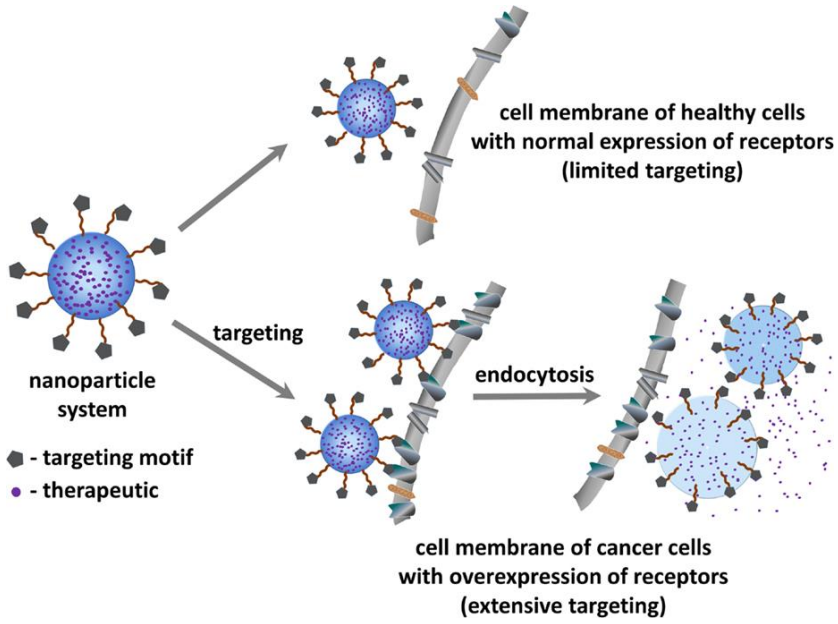

Figure 1.4. Selective binding of targeting nanocarrier to the cancer cells via receptors [10].

In active tumor targeting, targeting ligands are bound to the nanocarriers and these ligands have high affinity to attach to the receptors which are found in higher amounts on the surface of the cancer cells than that of the healthy cells. With this method, high local concentration of the drug at the surface of the targeted cells can be obtained. There are mainly two types of active targeting: One of them is targeting of cancer cells, the other one is targeting of tumorous endothelium.

First active targeting method is targeting of cancer cells. The cancer cells express some types of receptors on their surfaces more than healthy tissue cells. The nanocarriers are designed to have the targeting ligands of these specific receptors so that drug carrying nanostructures are selectively taken into the cancer cells by receptor-mediated endocytosis. There are some examples of the structures which are used in targeting cancer cells. They are transferrin, folate, glycoprotein and epidermal growth factor receptors.

Second active targeting method is targeting of tumoral endothelium. The tumoral endothelium is mainly responsible for neovascularization and angiogenesis which is new vein and capillary formation to feed cancerous tissue. These endothelial cells express some kinds of

receptors more than healthy tissue endothelium. By taking advantage of this situation, the nanocarriers having a targeting group on them direct tumoral endothelium and aim to prevent feeding the tumor via killing the tumoral endothelial cells. There are some examples of the structures which are used in targeting tumoral endothelium. They are vascular endothelial growth factor (VEGF) receptors, $\alpha_v\beta_3$ integrin receptors (highly expressed in both tumor cells and angiogenic endothelial cells, vascular cell adhesion molecule-1 (VCAM-1) and matrix metalloproteases (MMPs) [10-11].

A nanocarrier functionalized with a targeting group which is appropriate to the receptors of the targeted cells is internalized via receptor-mediated endocytosis by the cell. After meeting of the receptor and a targeting group on the nanocarrier, the cell membrane engulfs the nanocarrier and a vesicle forms. The lysosome is integrated and the nanocarriers release their contents via destruction by enzymatic activity. An example of folate mediated targeting can be as seen in Figure 1.5.

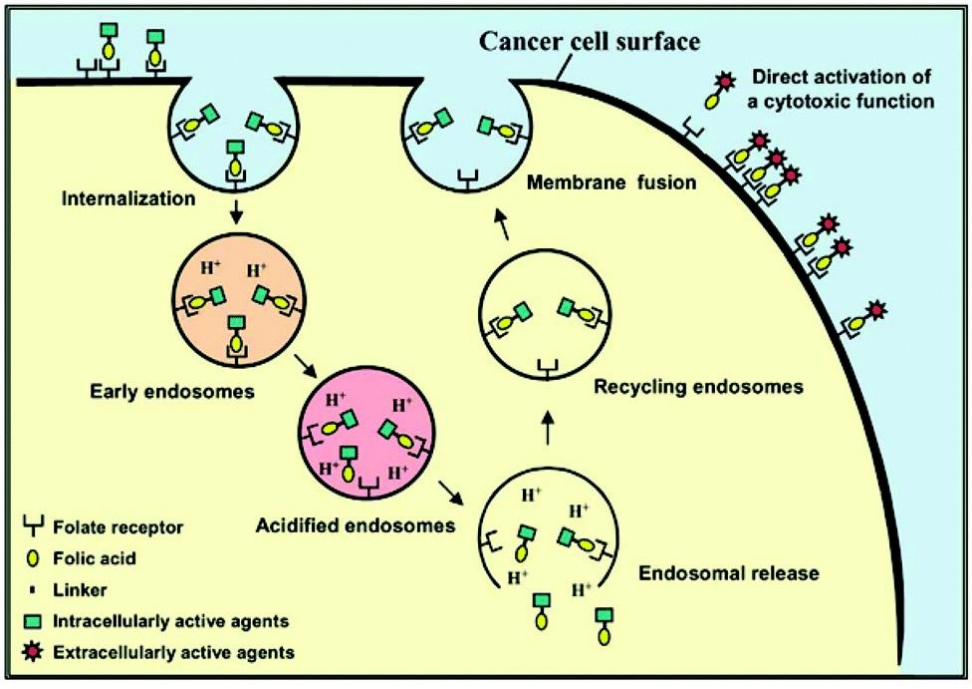

Figure 1.5. Endocytosis of folate group-functionalized quantum dots as nanocarriers [13].

1.2.3. Controlled Drug Release

In order to prevent harming the healthy cells with chemotherapy agents, release of the drug from the nanocarriers should occur only inside the tumor tissue or cancer cells. For this reason “controlled drug release” becomes a desired feature of the chemotherapy.

Controlled drug release provides stability to plasma drug concentration to stay between minimum effective concentration and maximum tolerated dose levels. As seen in Figure 1.6, when the drug is administered orally, plasma drug concentration reaches a quick peak but it drops quickly to well below minimum effective concentration requiring the next adminitration. However controlled administration results in a stable concentration at optimum level providing better results in treatment.

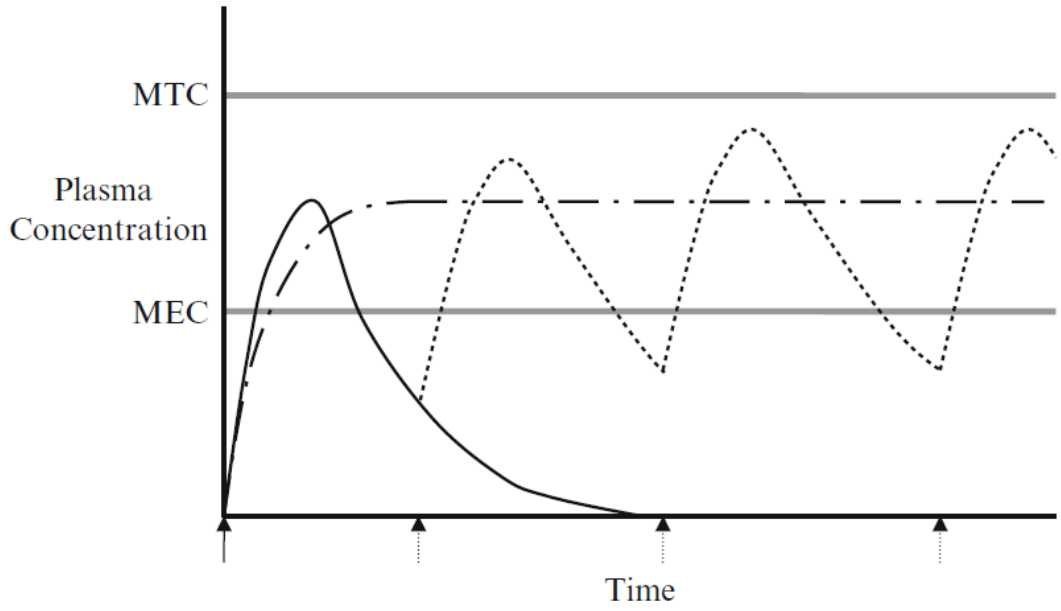

Figure 1.6. Plasma drug concentration in controlled drug release vs zero order oral release graph (MTC: Minimum toxic concentration, MEC: Minimum effective concentration) [14].

The drug can be loaded into the nanocarriers mainly in two methods. First method is to load physically, in which hydrophobic characteristic of the drug causes it to be encapsulated by the hydrophobic core of the nanocarrier. So the more hydrophobic the drug, the more the

encapsulation takes place. The second method is to covalently bind the drug to the nanocarriers. When the drug is non-conjugated to the nanocarriers but loaded with the help of only hydrophilic-hydrophobic interactions, the release of the drug from the nanocarriers cannot be controlled directly. A burst release of contents takes place as soon as the drug is administered and some of the drug cannot reach the tumor tissue. However, drug conjugated nanocarriers release their content in a controlled manner, such that an acid labile attachment between the drug and the nanocarrier breaks in only tumor tissue. Thanks to passive and active targeting, drug bearing nanocarriers directly affect the cancer cells and accumulate in the tumor tissue. Because the cancer tissues have more acidic pH (around 6.8) than healthy tissues, acid labile linkage between the drug and the nanocarrier breaks and drug becomes free only inside the tumor cells and kills only them [15].

According to Lee's study, a hydrophobic photosensitizer, chlorin e6 (Ce6), conjugated glycol-chitosan nanoparticles accumulate in different organs more than the non-conjugated analogs [16]. In the first group, Ce6 was physically loaded onto the hydrophobically-modified glycol chitosan nanoparticles (HGC). In the second group, the Ce6 was chemically conjugated to the glycol chitosan polymers, resulting in amphiphilic glycol chitosan-Ce6 conjugates. Compared to GC-Ce6, HGC-Ce6 showed a burst of drug release *in vitro*, 65% of physically loaded drug molecules were rapidly released from the nanoparticles within the first 5 h (Figure 1.7). When injected to tumor bearing mice, HGC-Ce6 did not accumulate much in tumor tissue, indicating the burst release of the physically loaded drug, while GC-Ce6 showed a prolonged circulation profile and a more efficient tumor accumulation (Figure 1.8a). Compared to GC-Ce6, HGC-Ce6 causes the accumulation of Ce6 in the tumor much more than the other organs, indicating that release of Ce6 in HGC-Ce6 begins before reaching the tumor and accumulates also in the healthy organs. However, conjugation of Ce6 as GC-Ce6 prevents early release, so the tumor seems the brightest due to the highest accumulation of Ce6 in the tumor (Figure 1.8b).

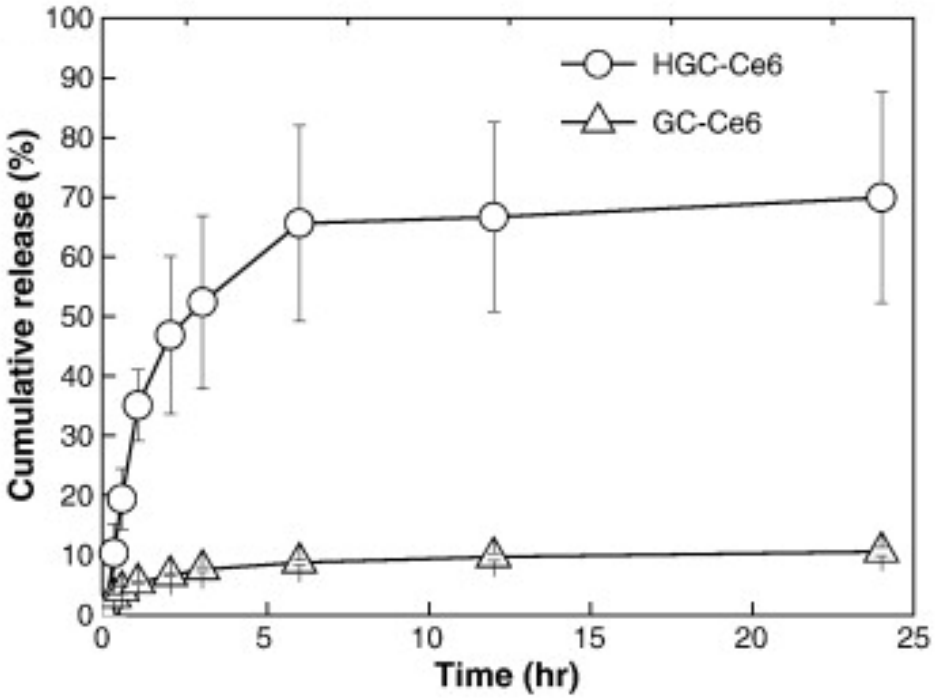

Figure 1.7. Cumulative release profiles of drug non-conjugated (HCG-Ce6) and conjugated (GC-Ce6) nanoparticles [16].

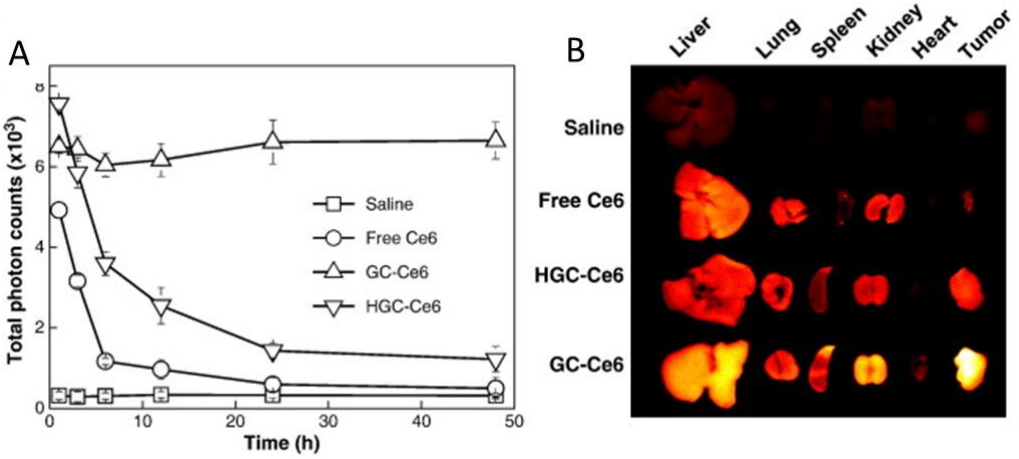

Figure 1.8. Comparison of drug non-conjugated (HCG-Ce6) and conjugated (GC-Ce6) nanoparticles (a) Quantification of *in vivo* tumor target specificity recorded as total photon counts (p/s/cm²/sr) of each tumor. (b) *Ex vivo* images of normal organs [16].

The first prevention method of burst drug release from nanocarriers is to conjugate the drug molecules to the nanocarriers as mentioned in Figure 1.7. There is also another method aiming to block burst release, which is to use a cross-linked matrix as a carrier. In the study of J. Chen and coworkers, photo-cross-linked micelles were prepared basing on poly(ethylene glycol)-hyperbranched poly(β-aminoester)s with acrylate group terminals (PEG-HBPAE-A) copolymers for intracellular delivery of dox. As seen in Figure 1.9, both cross-linked micelles (CLM) and non-cross-linked micelles (NCLM) release their content more at acidic pH = 5.0. However the release is less in the CLM compared to NCLM.

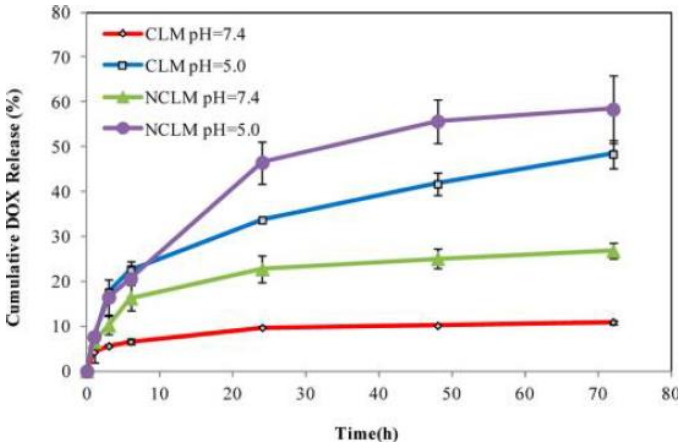

Figure 1.9. Cumulative release profiles of micelle constructs at different pH values [17].

1.2.4. The Relationship Between $\alpha_v\beta_3$ Integrin Receptor and cyclic-RGDfK Ligand

The integrin glycoproteins consist of different combinations and ratios of α and β subunits. The integrins are found on the cell surfaces and have a main role in cell adhesion to and the migration on some extracellular matrix proteins. $\alpha_v\beta_3$ type of integrin recognizes RGD (Arg-Gly-Asp) tripeptide which is present on extracellular matrix proteins such as fibronectin, vitronectin and collagen [10].

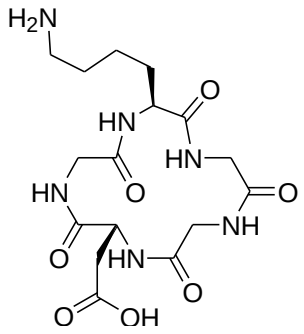

Figure 1.10. cRGD structure.

$\alpha_v\beta_3$ integrin is overexpressed on both of the endothelial cells and tumor cells in human breast, ovary and lung tumors. The reason of this situation is that $\alpha_v\beta_3$ integrins have a crucial role in angiogenesis. The enlarging tumor requires adequate supply of necessary nutrients and oxygen and new blood vessels provide them their such needs [19].

In order to directly target the cancer tissue in the patient body, RGD peptide can be chemically bound to the surfaces of the nanocarriers used in drug delivery systems. The nanocarriers having RGD peptide on their surfaces have a higher attachment affinity to the cancer tissue having more $\alpha_v\beta_3$ integrins on the cell membranes than the healthy tissue cells. Thus, the drug carrying nanostructures selectively kill cancer cells [20].

As explained in an article by Hirsjärvi and coworkers, cRGD grafted lipid nanocarriers showed higher binding and internalization to U87MG glioma cells compared to negative control and blank groups according to both flow cytometry and confocal microscopy images [21]. Also *in vivo* study indicated the same result. cRGD bearing lipid nanocarriers were accumulated in tumor tissue as seen in Figure 1.10 compared to the same nanocarriers decorated with a non-targeting cRAD peptide. Therefore, it is concluded that cRGD grafted lipid nanocarrier system provides benefits for tumor targeting.

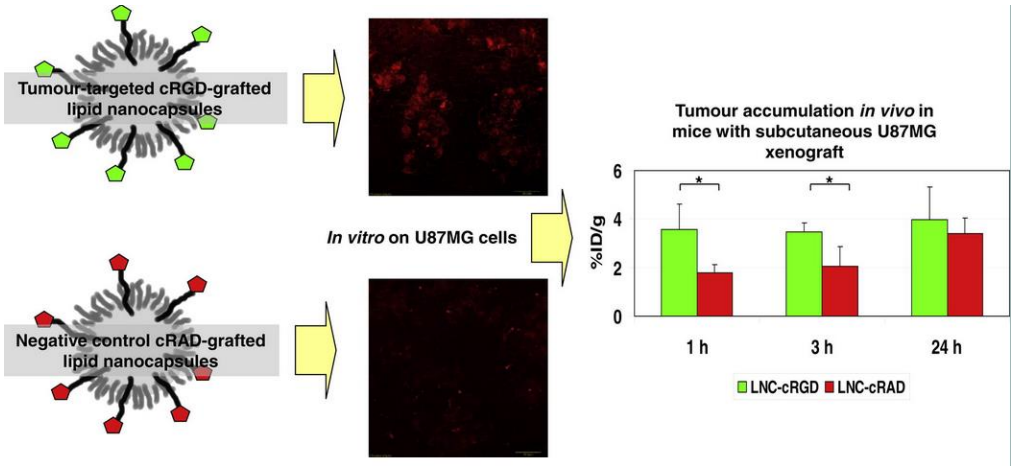

Figure 1.11. Increased internalization and tumor accumulation of LNCs with cRGD attachment [21].

According to a study by Murphy and coworkers, cRGDfK attached and dox loaded nanoparticles caused 15-fold increase in antimetastatic effect on pancreatic and renal cells without resulting in weight loss compared to free dox administration. Also selective apoptotic regions were detected in tumor vessels indicating this fluorescein-labeled nanoparticle system is able to prevent angiogenesis of cancer tissue as seen in Figure 1.12. This study shows that targeting $\alpha_v\beta_3$ integrin proteins which are extensively found on cancer tissue vessels and treatment of specific cancer cell types could be possible via utilization of cRGD ligand on the nanoparticle system.

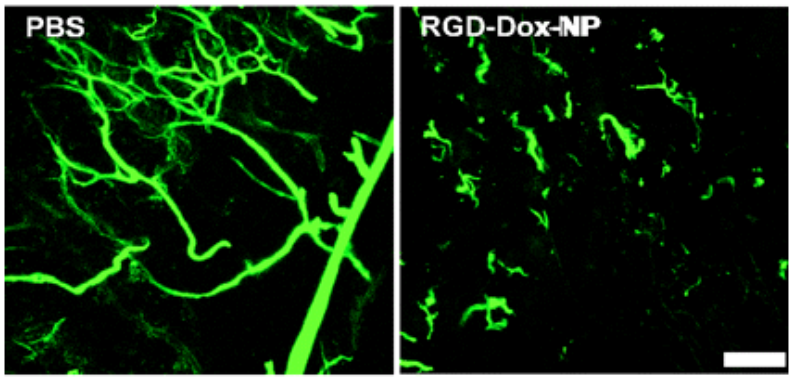

Figure 1.12. Prevention of angiogenesis due to RGD attached fluorescein-labeled nanoparticles [22].

1.3. Nanocarriers

In order to overcome the side effects and to reduce the handicaps of chemotherapy, some nano structures are chemically being established. The aim is to deliver these non-hazardous nanocarriers to the relevant area of the body of the patient with different mechanisms. Liposomes, dendrimers, polymers, nanoparticles and micelles are some examples of these nanocarriers, most of which are much more efficient than free chemotherapy drugs in terms of prevention of side effects, increasing the efficiancy and overcoming the disadvantages of chemotherapy.

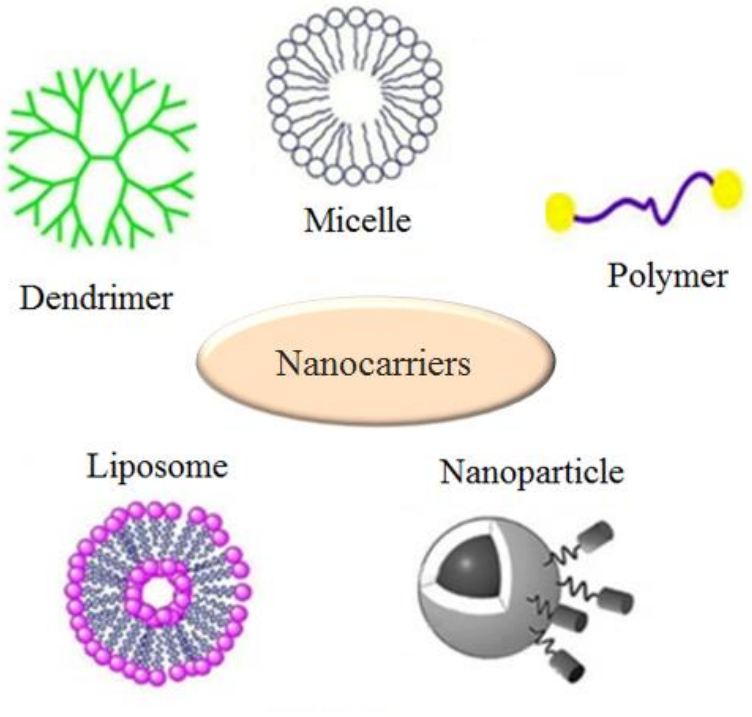

Figure 1.13. Some examples to nanocarriers [23].

1.3.1. Polymeric Nanoparticles

The chemotherapy agents have many disadvantages and side effects. One example of these problems is that most of the drugs have low water solubility. In order to reach the effective concentration of the drug in the blood, high amount of drug has to be administrated to the patient and this causes toxicity. Another example is the short circulation time of the drug in the patient body and its rapid renal clearance because of the tiny size of the drug.

Because it is cleared from the blood fast, it cannot be effective enough to kill high number of cancer cells. Also the chemotherapeutic drugs are not able to selectively kill only cancer cells. They are toxic to the healthy cells as well. These problems are the focus of most current studies [24].

In order to overcome these problems, new drug delivery systems are being developed. Polymeric nanoparticles are one of these systems. PLGA (poly-D,L-lactide-co-glycolide), PLA (polylactic acid), chitosan and gelatin are some examples used in nanoparticle formation.

Polymeric nanoparticle usage has many advantages. First of all, they are easily and cheaply produced with a variety of methods. Stability of the volatile drugs is increased by polymeric nanoparticles. Also effectiveness of the therapeutic agents increases via development over oral or intravenous administration. With the help of polymeric nanoparticles, it is possible to reach a higher concentration of the drug in corresponding body region. With these advantageous properties, polymeric nanoparticles are good candidates for usage in drug delivery and tissue engineering [25].

Besides the fact that polymeric nanoparticles are non-toxic to living cells, they have been used as good drug carriers that increase the efficiency of the drug in killing the cancer cells when applied *in vitro*. As seen in Figure 1.14, PLA NPs without drug have no toxic effect on the cells and dox grafted PLA NPs cause lower cell viability than free drug [26].

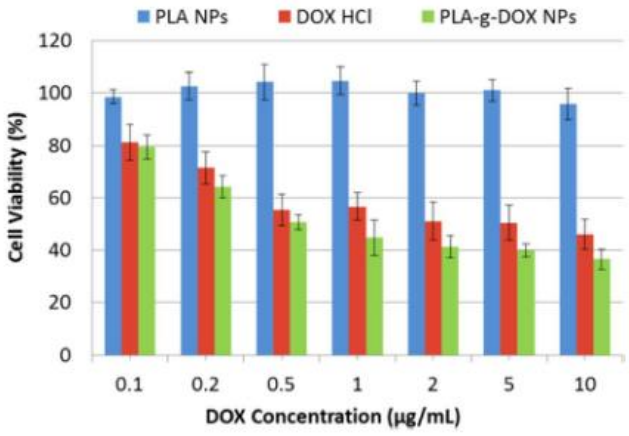

Figure 1.14. The positive effect of PLA NPs on reduction in cell viability [26].

1.3.2. Nanoparticle Preparation Techniques

There are a variety of biodegradable nanoparticle preparation techniques. Solvent evaporation, emulsification/solvent diffusion, salting out, dialysis, supercritical fluid technology, emulsion polymerization, interfacial polymerization and nanoprecipitation are the main methods for polymeric nanoparticle preparation. Different methods can be utilized according to the polymer type and the nanoparticle type wanted to be obtained.

In the general view, water-insoluble polymers are used as building blocks of nanoparticles. PLA, PCL and PLGA are some examples of these types of polymers. Rapid diffusion of the organic solvent into water causes decrease in interfacial tension between the solvent and water, thus small droplets of the solvent form a spherical accumulation of the polymer [27]. As an important advantage of this method, a hydrophobic core is built inside the nanoparticles, which is good for encapsulating hydrophobic drugs like most of the chemotherapy agents, as seen in Figure 1.13 [28-29]. This method is defined as nanoprecipitation which is one of the polymeric nanoparticle formation methods.

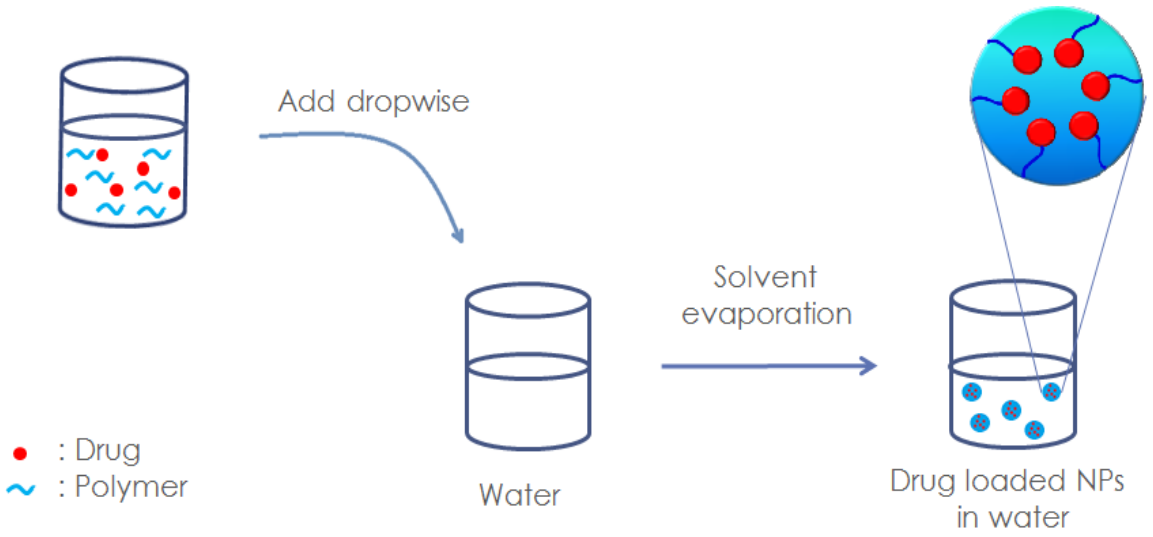

Figure 1.15. Nanoprecipitation.

Most of the polymeric NPs are biodegradable. After they release their contents inside the tumor cells, the polymer molecules composing them are degraded into smaller and harmless

structures with the degradation enzymes inside the lysosome. By this way the patient body gets rid of foreign structures without causing any side effect.

Besides physically doping the drug molecule to the nanoparticles with the help of hydrophobicity of the drug, chemically binding them to the polymer molecules is also possible. By this way, encapsulation efficiency of the drug can be increased because stability of the drug inside the nanoparticle core is enhanced by prevention of the early diffusion of the drug to the outside of the nanoparticles [30].

1.4. Ring-Opening Polymerization

The ring-opening polymerization (ROP) is a kind of chain-growth polymerization. In this polymerization, the terminal end of a polymer chain acts as a reactive center where further cyclic monomers can react via opening its ring and generate a longer polymer chain. The propagating center can be radical, anionic or cationic. Some examples of polymers obtained by this method can be seen in Figure 1.16.

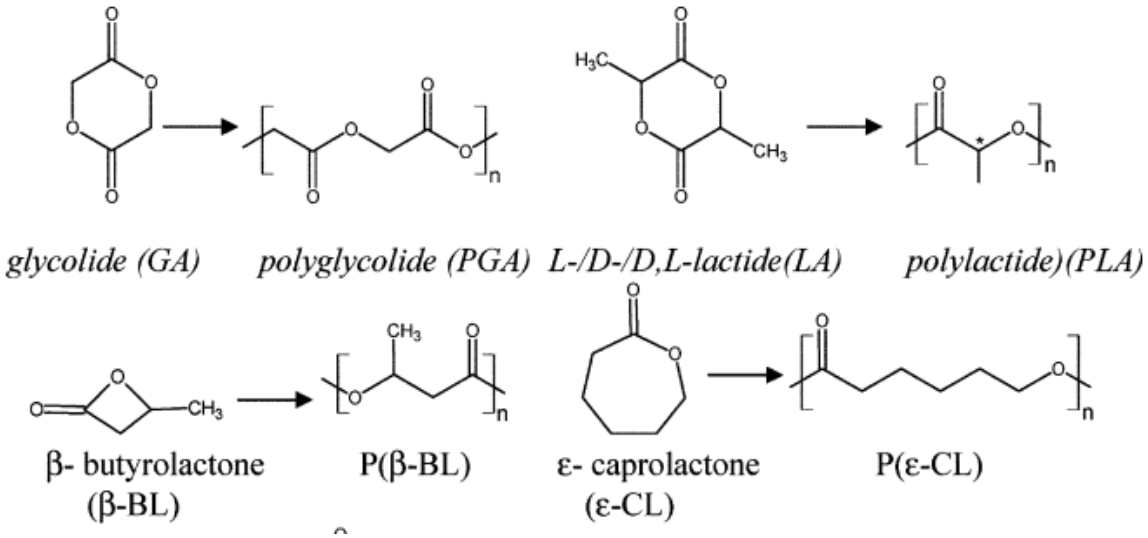

Figure 1.16. Ring opening polymerization [31].

1.5. Diels-Alder Reaction

Diels-Alder (DA) reaction is the [4+2] cycloaddition of a conjugated diene and a dienophile that involves the 4 π-electrons of the diene and 2 π-electrons of the dienophile (Figure 1.17). In this reaction new σ-bonds are formed which are more stable than the π-bonds. Diels-Alder reaction is widely used in synthetic organic chemistry due to its high yield and lack of side products [32].

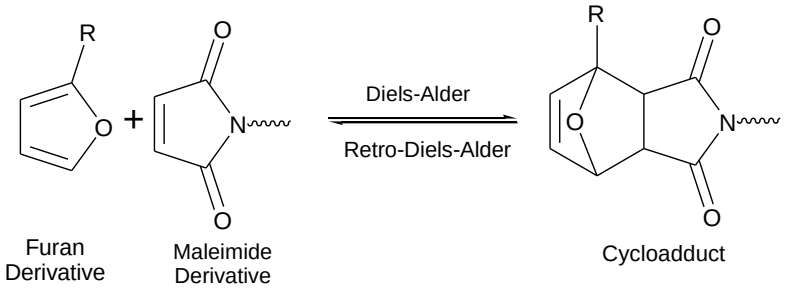

Figure 1.17. Diels-Alder reaction.

The reverse reaction is named as retro Diels-Alder reaction (rDA). It is possible to shift the reaction backwards only by increasing the heat. This property of Diels-Alder reaction makes it useful for thermoreversible systems.

Diels-Alder reactions can be used on nanoparticle systems. Surface functionalization via Diels-Alder reaction in Engel's study provides the information that reactivity of the molecules which are attached to the particles depends on steric crowding (Figure 1.18).

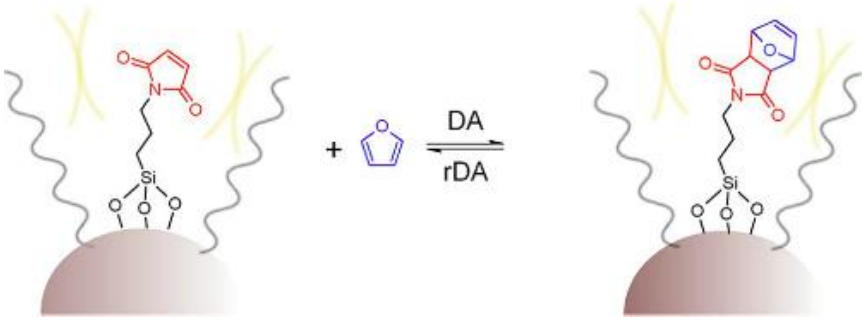

Figure 1.18. Diels-Alder reaction on nanoparticle surface [33].

In a study by Shoichet and coworkers (Figure 1.19.); poly(TMCC-*co*-LA)-*g*-PEG-furan copolymer was used as the building blocks of the nanoparticles to make it possible to attach maleimide-modified antibodies as targeting groups onto the surface of the nanoparticles. The polymer they used was biodegradable and biocompatible, which renders the immuno-nanoparticles eligible to use *in vivo* and *in vitro* studies besides investigation of targeting via antibodies.

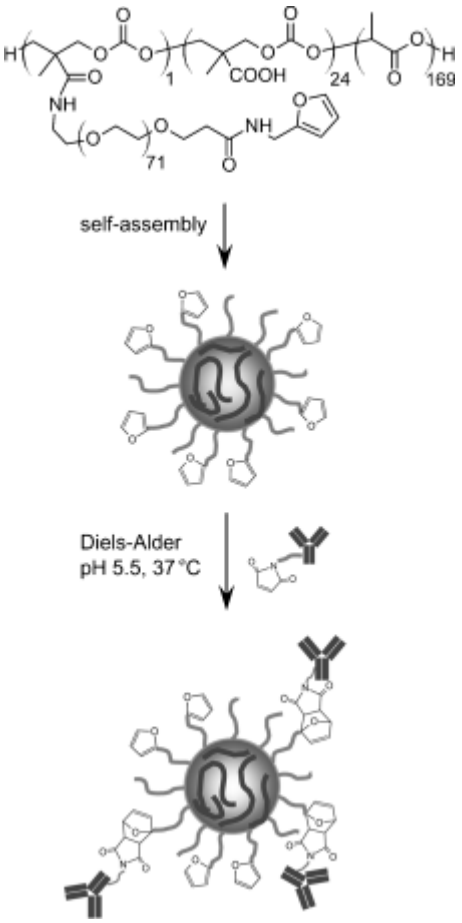

Figure 1.19. Self-assembly of furan-bearing copolymers to form nanoparticles and attachment of maleimide-modified antigens via Diels-Alder chemistry [34].

The building blocks of the nanocarriers have an important effect on drug release profiles, both the speed of release and total amount of drug released. If a hydrophilic polymer participates in the construct, the nanocarriers lose their packed structures by increasing the pore sizes on the surface causing an increase in the released amount.

According to Tobio and coworker's study, a model antigen, ^{125}I-radiolabeled tetanus toxoid (TT), was encapsulated in PLA and PLA-PEG nanoparticles. The *in vivo* experiments showed that, after oral administration of radioactive antigen loaded nanoparticles to rats, the levels of encapsulated radioactive antigen in the blood stream and lymphatics were higher for PLA-PEG nanoparticles than for PLA nanoparticles. The total release percent were obviously increased both in gastric fluid and intestinal fluid (Figure 1.20).

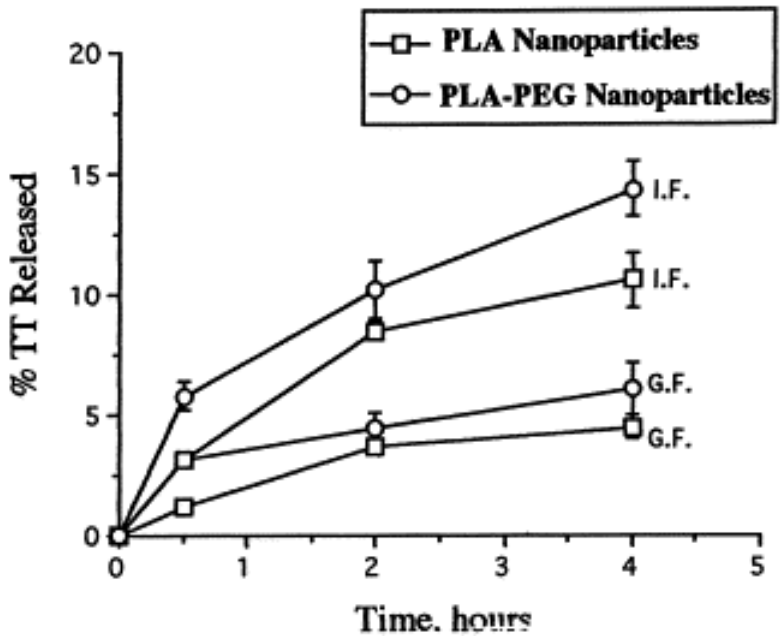

Figure 1.20. *In vitro* release of ^{125}I-radiolabeled TT from PLA and PLA-PEG in gastric (G.F.) and intestinal fluids (I.F.) [35].

In this study, drug loaded polymeric nanoparticles are designed as a controlled drug delivery system. The building block polymer is synthesized with ring opening polymerization. The drug molecules and the targeting groups are attached to the nanoparticles with Diels-Alder reaction. This nanoparticle system can be further used *in vivo* studies and possible successful results can be explained with passive and active targeting concepts.

2. AIM OF THE STUDY

The aim of this study is to design a universal biodegradable polymeric nanoparticle based drug delivery system that can be utilized to transport drugs to cancerous tissue via both passive and active targeting. A modular nanoparticle system that would allow facile conjugation of drugs to minimize burst and prolong release, along with facile attachment of targeting units is developed (Figure 2.1). Ring opening polymerization in the presence of a novel reactive monomer was used to obtain biodegradable polymer, a furan-bearing PLA-carbonate copolymer. Polymeric nanoparticles were prepared using this copolymer with nanoprecipitation method. Doxorubicin was used as drug to be loaded into the nanoparticles. The loading was done either physically based on only hydrophilic-hydrophobic interactions between the nanoparticle core and the drug or chemically by binding the drug to the polymer molecules via Diels-Alder reaction after modification of the drug with a maleimide unit. In particular, the Diels-Alder reaction, an efficient conjugation reaction was utilized to avoid any possible toxicity arising from residual metal impurities. Importantly, the drug release characteristics of PLA nanoparticles were tuned by varying the hydrophilicity of the nanoparticles through conjugation of maleimide-containing polyethylene glycol units (PEG). A peptide based targeting group, cRGDfK-containing molecules were attached to these nanoparticles with Diels-Alder reaction to investigate potential targeting of MDA-MB 231 breast cancer cells overexpressing integrin receptors.

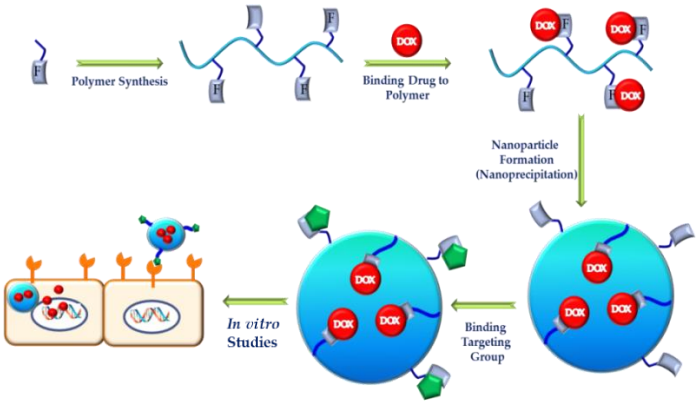

Figure 2.1. General scheme of the project.

3. RESULTS AND DISCUSSION

3.1. The General Method for Preparation of the First Generation Nanoparticles

First generation polymeric nanoparticles were fabricated using nanoprecipitation of furan-bearing polylactide copolymers. Dox-encapsulated PLA nanoparticles and maleimide-Dox-conjugated furan-bearing PLA nanoparticles are referred as first generation nanoparticles. While non-functional group bearing PLA polymer and dox were obtained from commercial sources, furan-bearing PLA polymer and maleimide-containing dox were synthesized.

3.1.1. Synthesis of Furan-Bearing PLA-Carbonate Copolymer

As a building block of nanoparticles, furan-bearing PLA-carbonate copolymer was synthesized. The reason of using such a copolymer was its biodegradable nature along with availability of pendant furan groups which would allow attachment of maleimide-bearing drugs targeting groups. Furan group-bearing polylactide-carbonate copolymer (**3**) was synthesized by using a furan-bearing cyclic carbonate (**2**) and L-lactide (**1**) as starting materials in the presence of benzyl alcohol, 1-(3,5-bis(trifluoromethyl)phenyl)-3-cyclohexyl-thiourea (TU) and 1,8-diazabicycloundec-7-ene (DBU) in CH_2Cl_2 at room temperature. The obtained copolymer was purified via precipitation in 1:1 diethyl ether: methanol mixture.

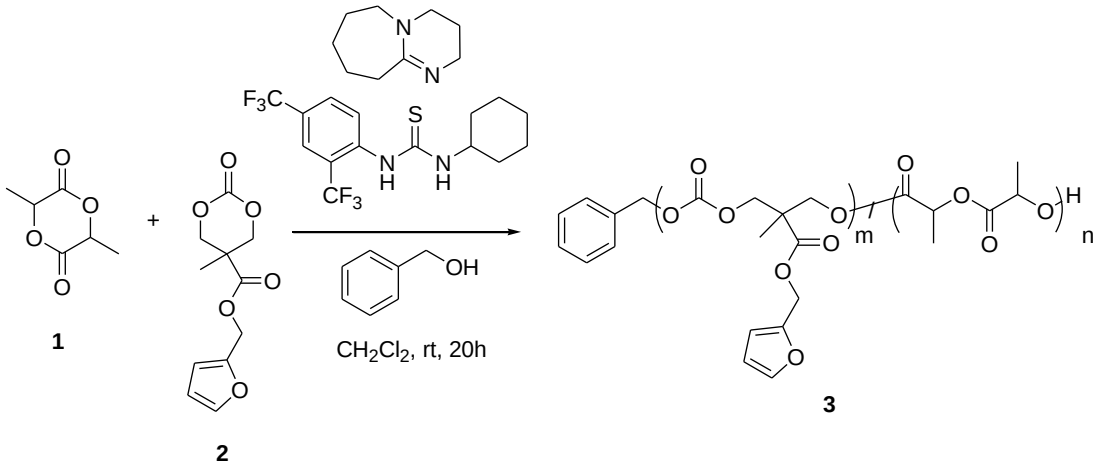

Figure 3.1. Synthesis of furan group-bearing polylactide-carbonate copolymer.

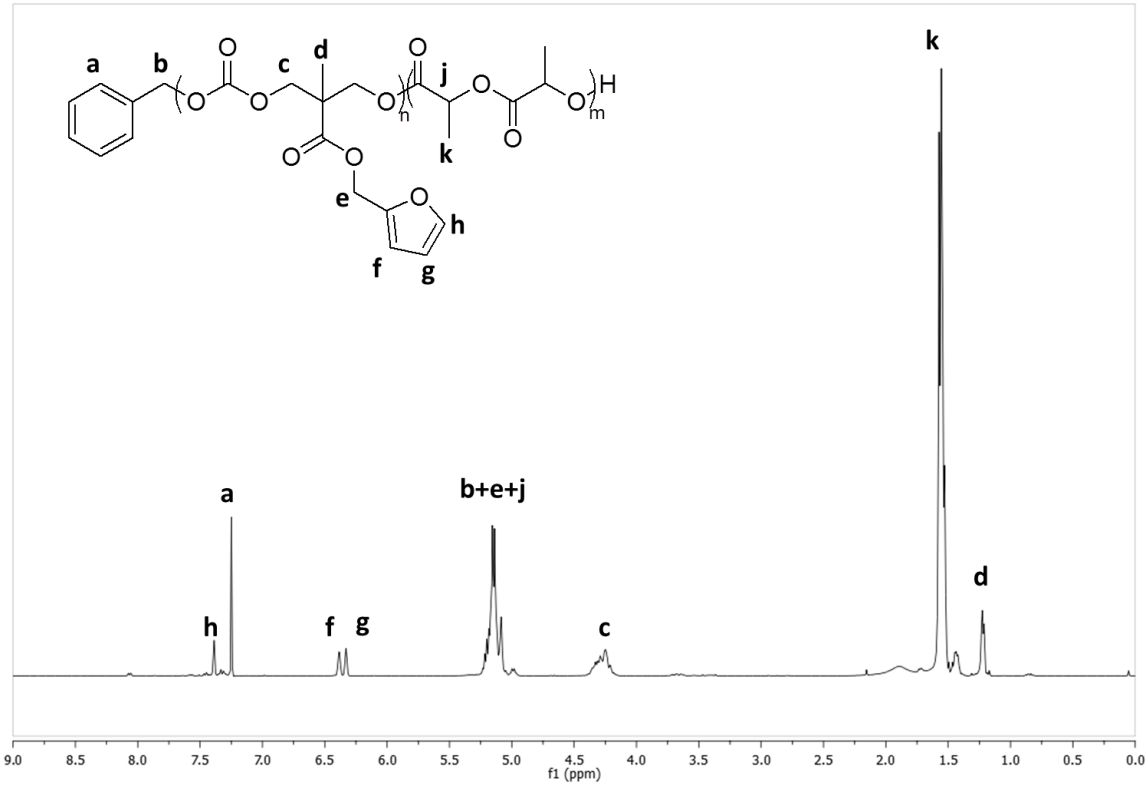

Figure 3.2. ^{1}HNMR spectra of furan-bearing PLA-carbonate copolymer (**3)**.

The chemical composition and purity of obtained copolymer **3** was established using ^{1}HNMR spectroscopy. Proton resonances corresponding to-H_d protons are observed near 1.22 ppm as a singlet. Resonances from H_k protons of methyl groups appear between 1.50-1.64 ppm as a multiplet. Resonances from H_c are seen at 4.25 ppm, and H_b, H_e and H_j are detected between 5.25 and 5.25 ppm as a multiplet. Furan group hydrogens H_g and H_f are observed as singlets at 6.33 and 6.38 ppm respectively. Benzyl group protons H_a are seen as a singlet at 7.25 ppm. H_h protons are seen as a singlet at 7.29 ppm. The moderately high number average molecular weight and a monomodal molecular weight distribution of the copolymer was established using size exclusion chromatography (M_n = 12kDa, M_w/M_n = 1.19, Figure 3.3).

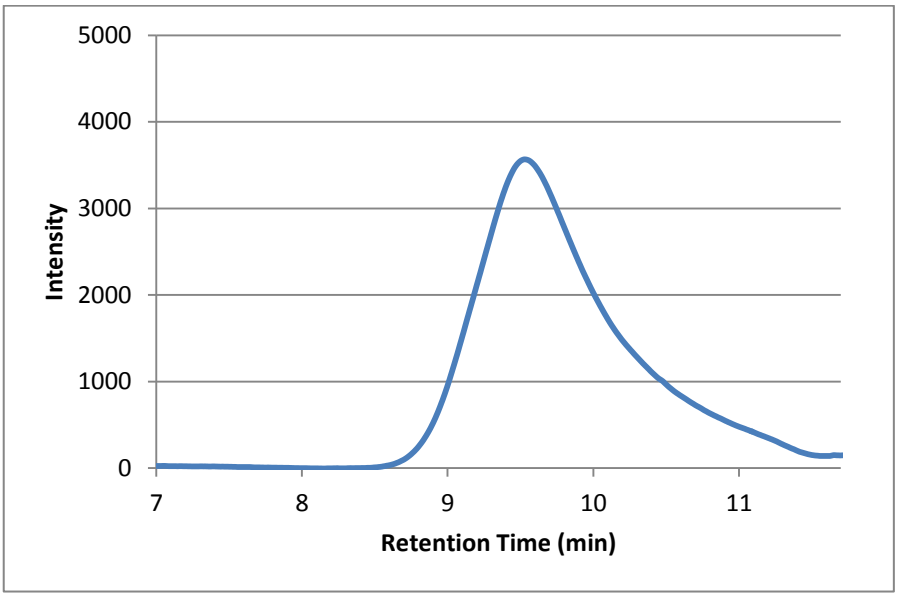

Figure 3.3. GPC curve of furan-bearing PLA-carbonate copolymer (**3**).

3.1.2. Synthesis of Maleimide-Containing Doxorubicin

In order to modulate the release of the encapsulated drug from the nanoparticles, the drug needs to be chemically bound to the nanoparticles. Since we utilize a furan-maleimide based conjugation reaction for the attachment of the drug, a maleimide containing linker is incorporated into the drug. Commercially available N-ε-maleimidocaproic acid hydrazide (EMCH) (**5**) linker is attached to Dox (**4**) with a hydrazone bond as shown in Figure 3.4. This hydrazone bond is acid labile and easily broken around pH= 5.4 like inside cancerous cells, so drug becomes free predominantly inside the cancer cells.

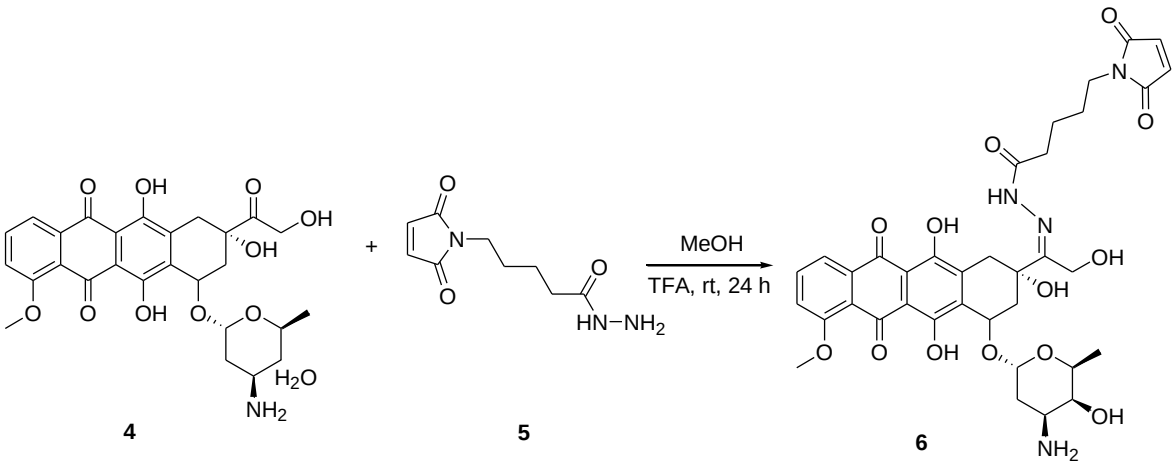

Figure 3.4. Attachment of maleimide group containing linker to Dox.

FT-IR spectra of **6** was obtained where a shift in that peaks corresponding to the carbonyl shifts from 1726.07 cm^{-1} to 1667.41 because of the amide bond formation (Figure 3.5).

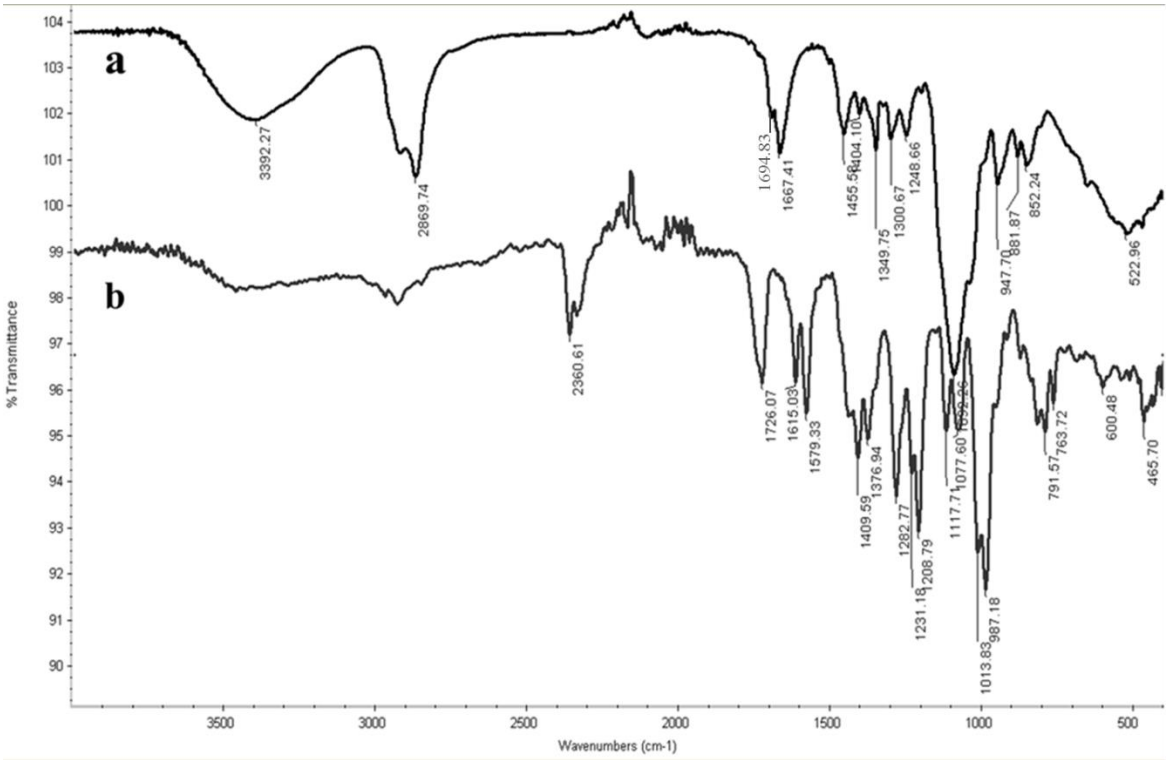

Figure 3.5. FT-IR Spectra of Dox-EMCH (a) and Dox (b).

3.1.3. Synthesis of First Generation Nanoparticles

In nanoparticle formation, nanoprecipitation method was used. This method includes precipitation of the dissolved polymers in non-solvent which is miscible with the solvent [36]. In this study different combinations of commercially available PLA, furan-bearing PLA-carbonate copolymer (M_n = 14 700 Da, PDI=1.3), were used as building blocks of the nanoparticles. Dox.HCl, dox and maleimide linker bearing-dox were used as drugs/prodrugs as either encapsulated in or conjugated to the nanoparticle during the nanoprecipitation process.

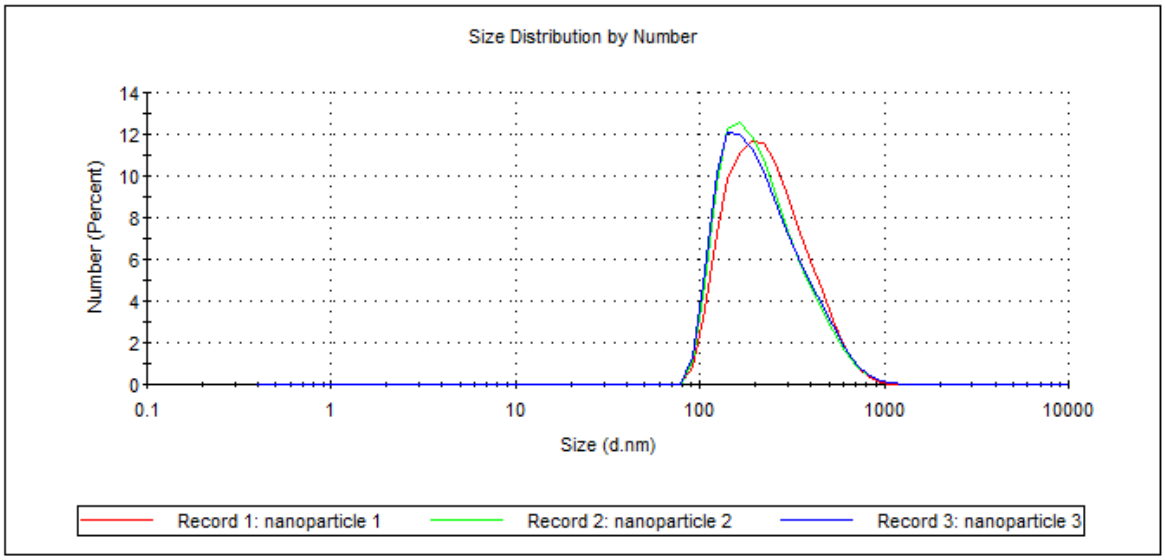

Figure 3.6. DLS curve of NP 1.

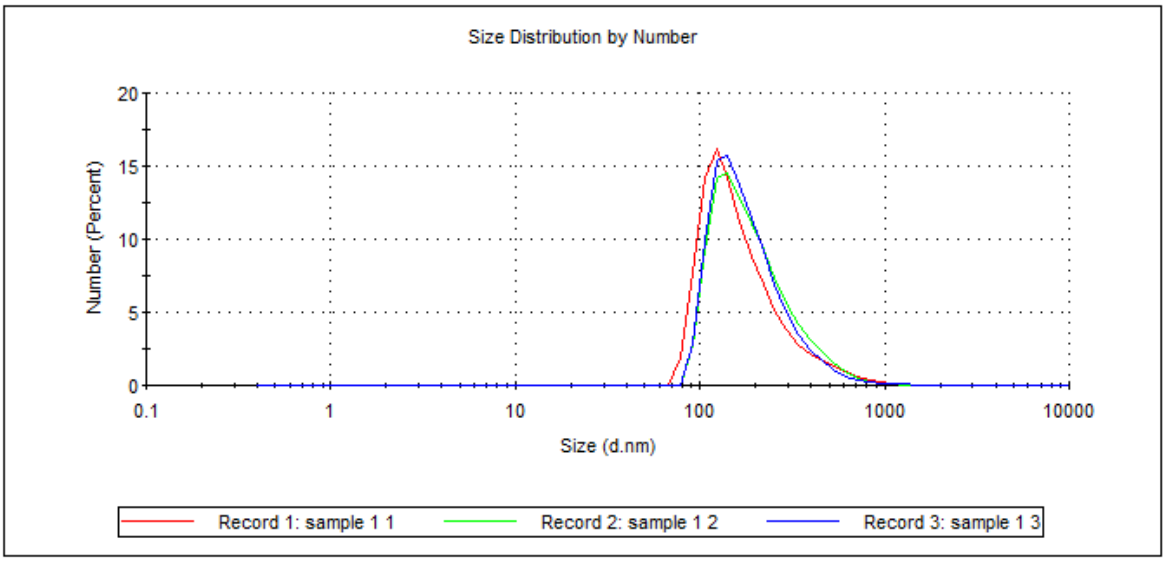

Figure 3.7. DLS curve of NP 2.

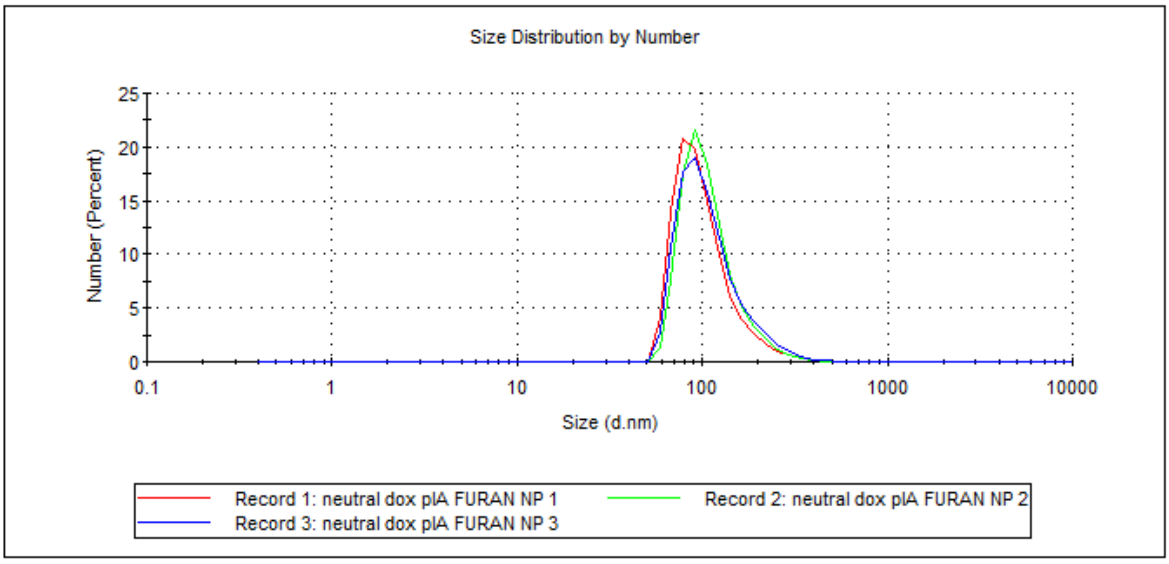

Figure 3.8. DLS curve of NP 3.

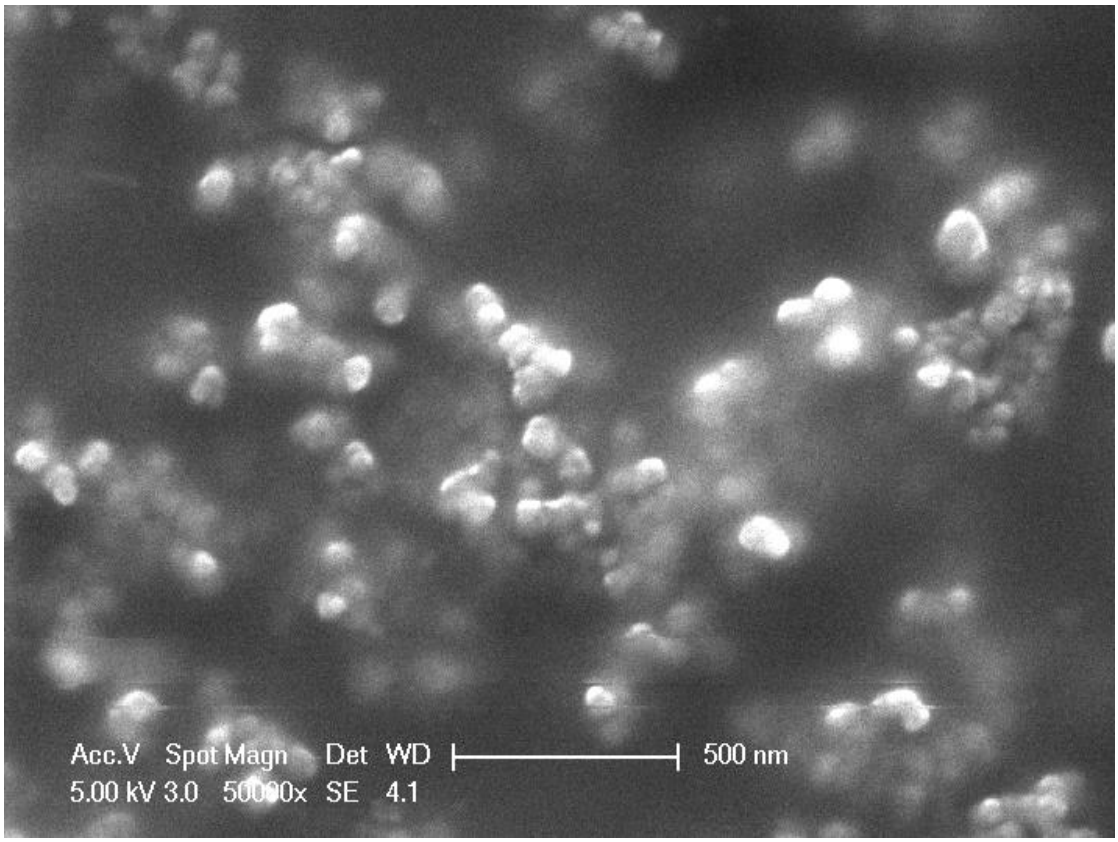

Figure 3.9. SEM image of NPs.

Initially, acetone was used as a water-miscible solvent to formulate NP 1-9 batches. Polymers and the drug are dissolved in acetone and added to water. It was observed that even though the entire polymer gets dissolved, some of the drug does not. Increasing the amount of acetone was not a good option because the solvent needs to evaporate at a moderately rapid rate to ensure the formation of the nanoparticles. In order to encapsulate more drug, the solvent was changed to tetrahydrofuran (THF), another water miscible organic solvent. A solution of polymer and drug in THF was added to distilled water drop-wise while stirring. After evaporation of the organic solvent, the solution appears to be pink and turbid which indicates nanoparticle formation. Particle size measurements using dynamic light scattering (DLS) measurements were obtained to confirm particle formation and determine their size.

In order to remove the free drug and free polymers, ultracentrifugation is done with Amicon Millipore centrifuge tubes in which the nanoparticles are stuck onto the membrane

and cannot be re-suspended back. Then normal centrifugation is done with centrifuge tubes and precipitated nanoparticles are re-suspended easily. Their DLS data is obtained to compare them with the DLS measurements of the NP solution before the centrifuge to reveal that particles did not agglomerate during this purification process.

After purifying the NP solution from free drug by centrifugation, encapsulated drug amount is calculated with the help of fluorescence spectroscopy (FS). The absorbance value obtained from FS is located in calibration curve equation and the weight of encapsulated drug is calculated. This value is used in encapsulation efficiency (EE) equation. EE of the PLA nanoparticles are calculated as follows:

$$EE\ \% = 100\ \text{x}\ \frac{\text{Encapsulated weight of the drug}}{\text{Initial added weight of the drug}}$$

Table 3.1. Different combinations of the polymer type, drug type and targeting group in various batches of first generation NPs.

	Drug			Polymer		DLS Measurements			
NP #	Dox.HCl	Dox	Dox-EMCH	PLA	PLA-Furan	Size (nm)	PDI	EE (%)	Wt %
1	+			+		255.5 ± 131.4	0.192	10.8 ± 5.7	0.27
2		+		+		188.4 ± 134.3	0.286	45.8 ± 7.9	1.15
3			+		+	104.3 ± 43.66	0.157	88.6 ± 14.5	2.21

NP 1 had Dox.HCl which was the more hydrophilic version of the drug. It had a higher tendency to go out of the hydrophobic core of the NP to very hydrophobic environment, water. Because of this facility, drug was not encapsulated into the NP with high efficiency (10.8 ± 5.7 %) (Table 3.1). Due to the hydrophobicity problem of the drug, it was neutralized and became more hydrophobic. With this new version of the drug NP 2-3 were formed. The drug preferred to stay in the hydrophobic core much more than NP 1 and has high encapsulation efficiency. Encapsulation efficiencies of NP 2-3 were 45.8 ± 7.9 and 88.6 ± 14.5 % respectively.

In order to increase the encapsulation efficiency more, drug and polymer structure is a little bit changed to form chemical bond between them. The drug is functionalized with maleimide linker (EMCH) and the polymer **3** is with furan group. So the drug and the polymer are able to bind each other via Diels-Alder reaction with these new functional groups as seen in Figure 3.10. NPs 7-12 are formed with these building blocks.

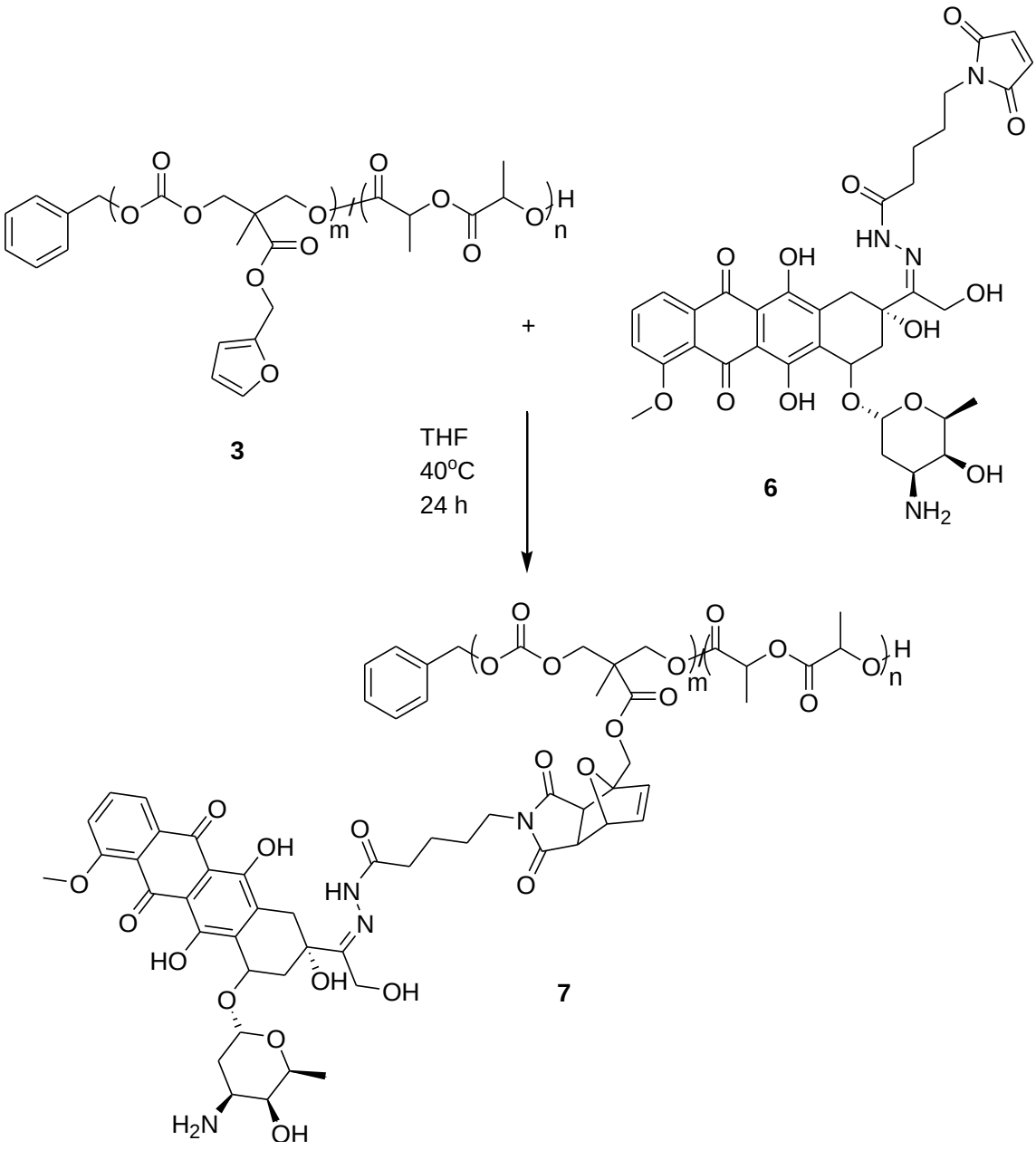

Figure 3.10. Dox attachment to PLA-carbonate copolymer **3** via Diels-Alder reaction.

3.1.4. Drug Release from First Generation Nanoparticles

Release of encapsulated drug was attempted under neutral and acidic conditions. The aim of these studies is to test the release behavior of the anticancer drug from the nanoparticle in acidic environment which mimics the cancer cell environment. No release of drug was observed at neutral environment (Figure 3.11) and under acidic conditions (Figure 3.12). The reason for this could be that NPs with PLA or furan bearing PLA-carbonate copolymer are highly packed. This situation prevents release of the drug from the nanoparticles due to lack of diffusion of water to the interior of the nanoparticle. It is needed to increase the hydrophilicity of the NPs enable the drug molecules go out of the NP core when it should release.

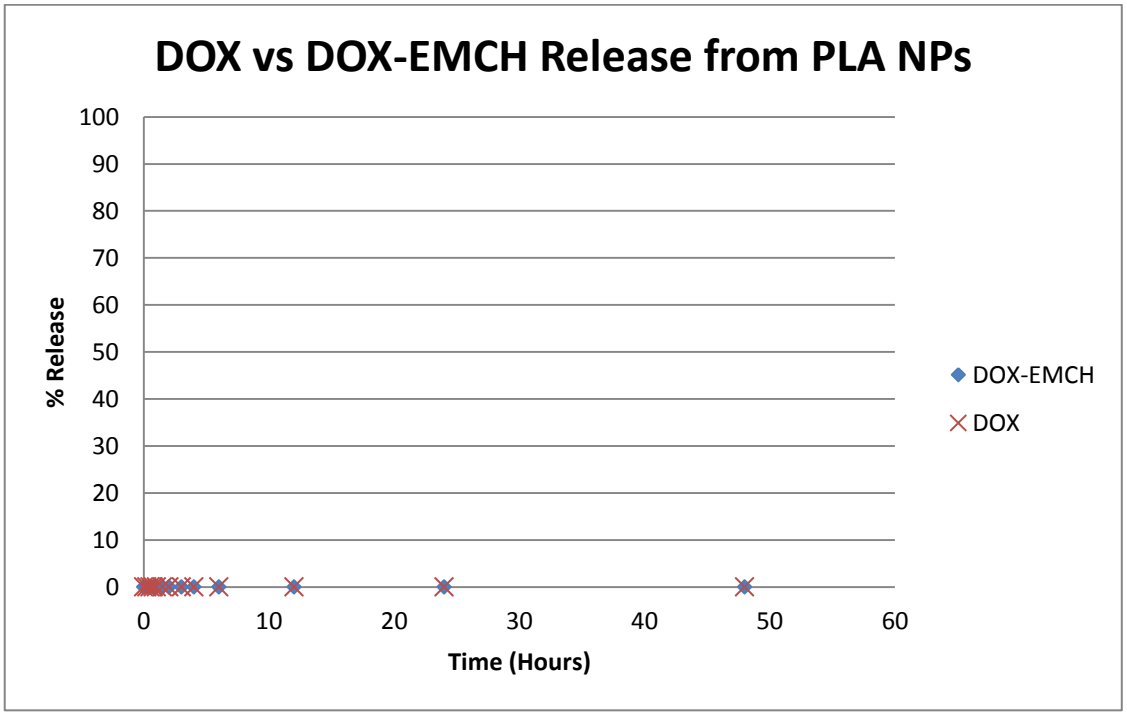

Figure 3.11. Release profiles of Dox and Dox-EMCH from PLA NPs at pH=7.4.

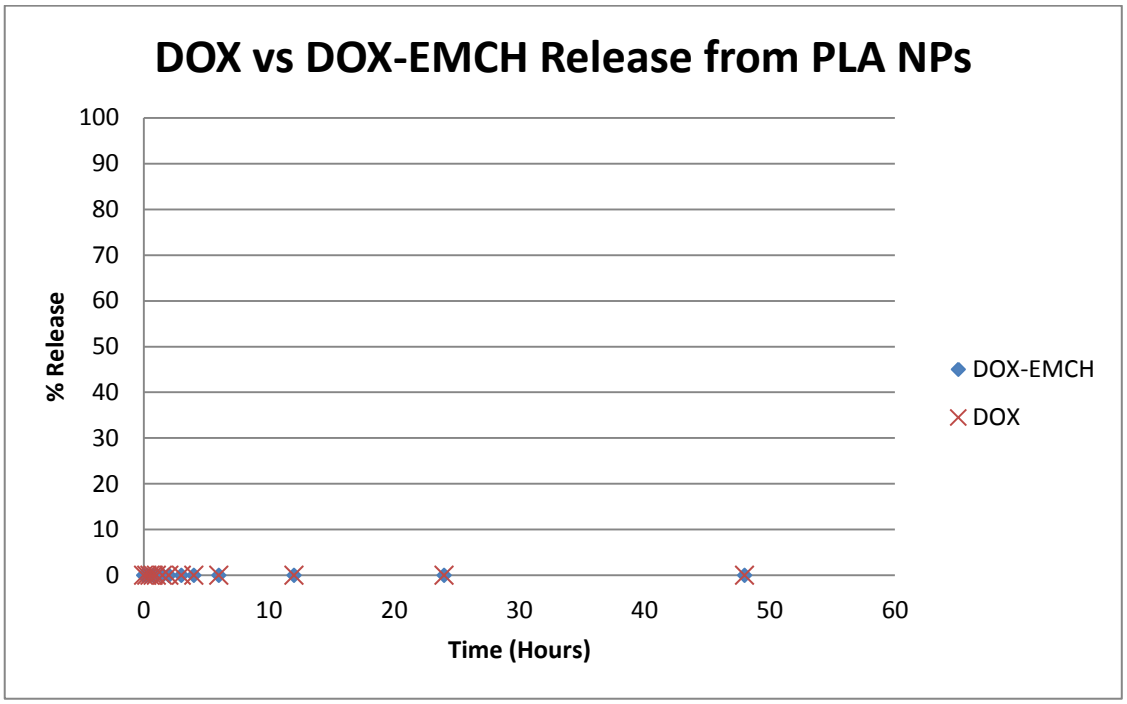

Figure 3.12. Release profiles of Dox and Dox-EMCH from PLA NPs at pH:5.4.

3.2. General Method for Preparation of Second Generation Nanoparticles

3.2.1. Synthesis of Mono-Maleimide PEG

In order to increase the hydrophilicity of outer surface of the drug containing nanoparticles, polyethylene glycol (PEG) chains were attached to polylactide-carbonate copolymer chemically during the nanoprecipitation process. This attachment procedure was done using the Diels-Alder reaction between furan groups of the polylactide-carbonate copolymer and maleimide groups of the PEG. For this reason commercially available polyethylene glycol monomethylether 750 (**8**) was used as a starting material and furan-protected maleimide group bearing alcohol (**11)** was attached to it (Figure 3.13).

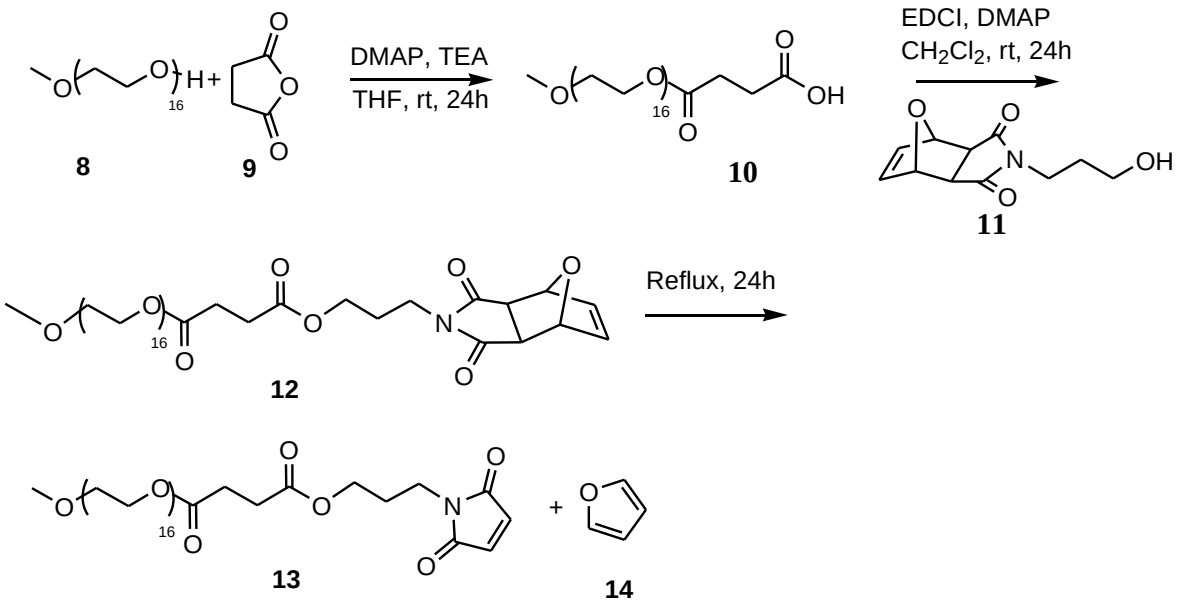

Figure 3.13. Synthesis of Mono-Maleimide PEG (**9**).

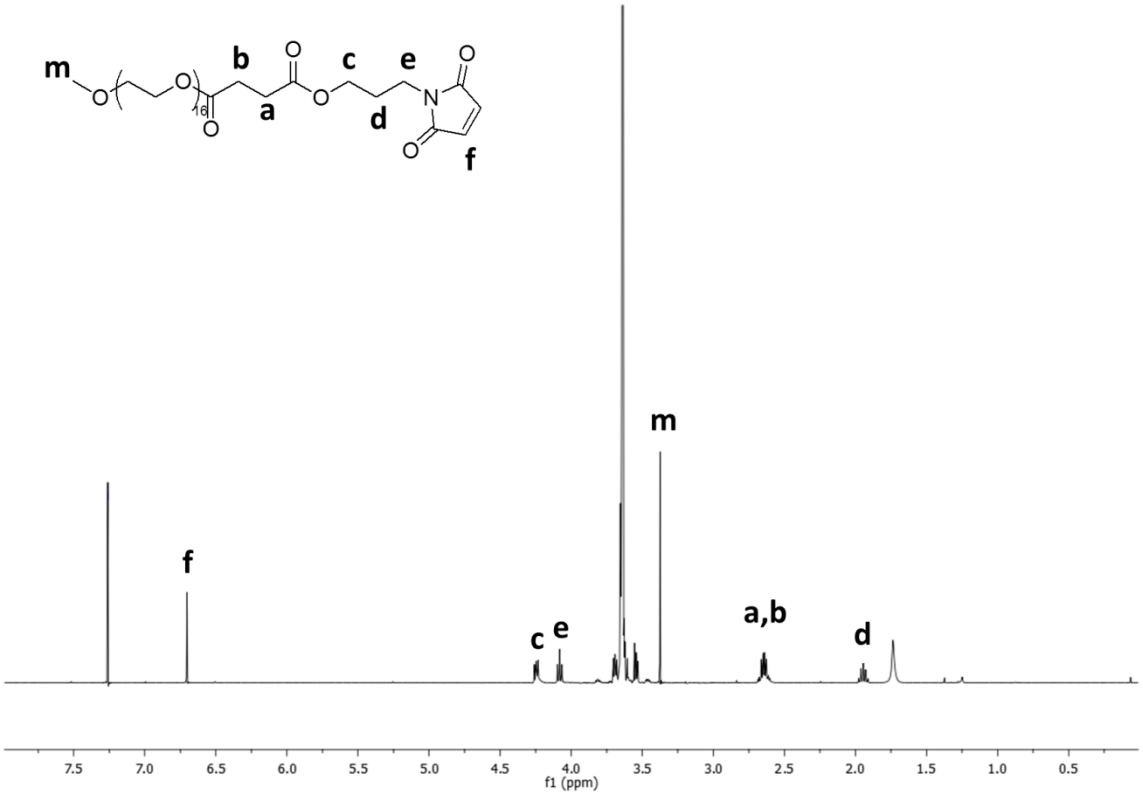

Figure 3.14. ^{1}H-NMR spectrum of Mono-Maleimide PEG (**13**).

The proton spectra of mono-maleimide PEG (**13**) can be seen in Figure 3.14. H_d protons are observed near 1.89 ppm as triplet of triplet. Both H_a and H_b protons are between 2.60-2.69 ppm as multiplet. H_m protons of methoxy group are seen at 3.35 ppm as a singlet. Between 3.41-3.82 ppm, there is a multiplet of polyethylene glycol hydrogens. H_e and H_c protons are observed as triplets at 4.03 and 4.22 ppm respectively. H_f protons are seen as a singlet at 6.71 ppm.

Nanoparticles (NP 4-9) formulated with PEG-maleimide contains a Diels-Alder adduct between maleimide group of the PEG and furan group of the PLA-carbonate copolymer (Figure 3.15). Also because PEG has a hydrophilic structure, it is expected to be generally at outer surfaces of the NPs but also can be expected to generate some hydrophilic domains inside the nanoparticle since it will be covalently bound to the hydrophocic carbonate copolymer. It can be expected that the increase in the amount of PEG will lead to formation of nanoparticles with slight increase in size. Increasing the hydrophilic component beyond a certain amount can be expected to impede the formation of stable nanoparticles. Various PEG:PLA ratios (1.1, 2:1, 3:1 and 4:1) were evaluated towards nanoparticle formation. As expected, beyond a 3:1 PEG:PLA ratio, NP structures were not obtained through nanoprecipitation.

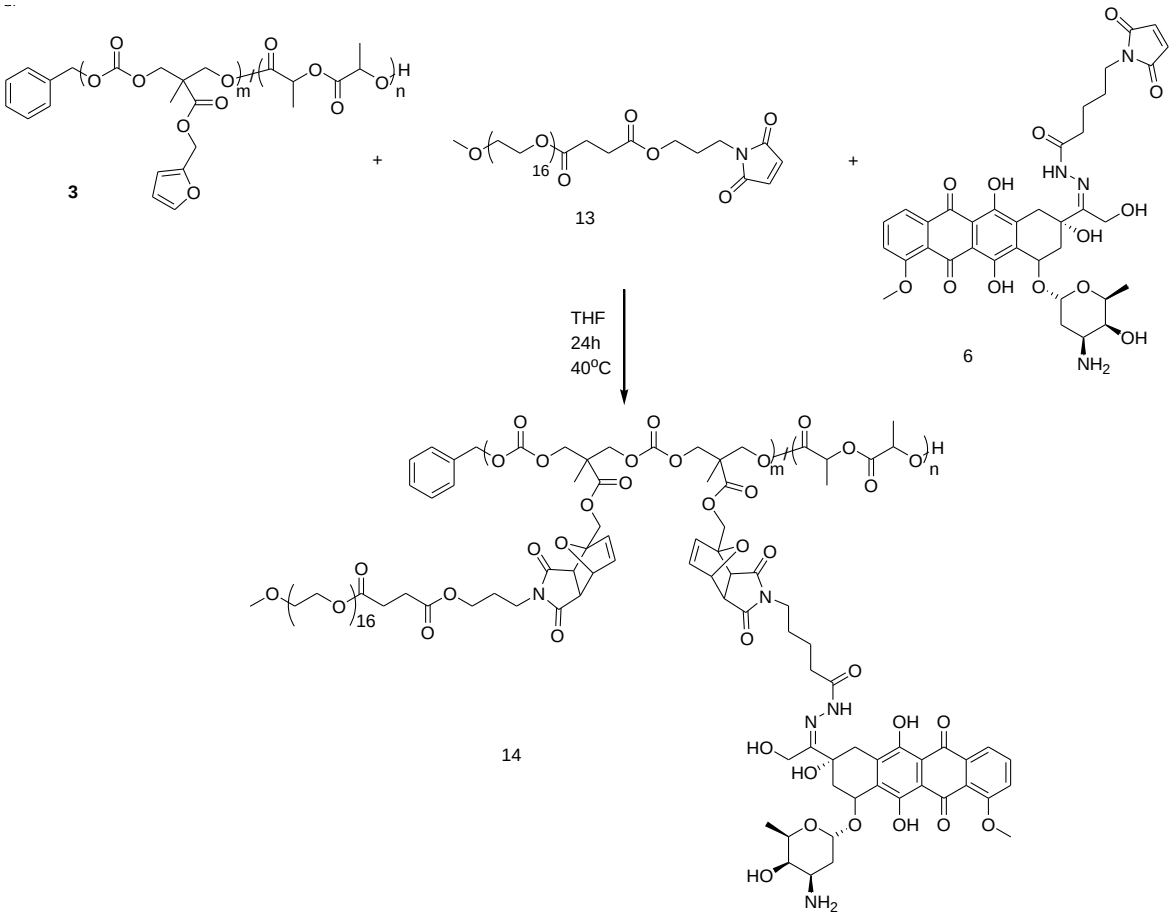

Figure 3.15. Mono-maleimide PEG (**13**) binding to PLA-carbonate copolymer (**3**) via Diels-Alder reaction.

Table 3.2. Different combinations of the polymer type, drug type and targeting group in various batches of second generation NPs.

	Drug		Polymer 1	Polymer 2	DLS Measurement			
NP #	Dox	Dox-EMCH	PLA-Furan	PEG-Maleimid	Size (nm)	PDI	EE (%)	Wt %
4	+		+	+	120.3 ± 36.33	0.034	34.8 ± 6.8	0.87
5	+		+	+	92.29 ± 35.31	0.153	30.7 ± 2.4	0.77
6	+		+	+	90.93 ± 49.41	0.260	20.1 ± 5.7	0.50
7		+	+	+	120.1 ± 64.58	0.187	70.8 ± 11.2	1.77
8		+	+	+	153.1 ± 92.6	0.270	64.4 ± 8.7	1.61
9		+	+	+	136.4 ± 72.93	0.186	41.0 ± 9.7	1.02

3.2.2. Drug Release from Second Generation Nanoparticles

After preparation, purification and characterization of the nanoparticles, release studies were done. The release studies are done in both 1 x PBS pH=7.4 and citrate buffer pH=5.4. If this system is used for *in vivo* studies, the nanoparticles cannot release their content in healthy tissues due to neutral pH but release only in cancerous tissues. Hence, side effect of the anticancer drug is diminished. The reason of utilizing acidic buffer is that hydrazone bond formed between the drug dox and its linker EMCH is broken in this acidic media and the drug becomes free. Similarly, cancer tissue has acidic environment, which causes breaking the hydrozone bond between the drug and the polymer to leak from the nanoparticle to the cancer tissue.

The release profiles of dox from both DENPs and DCNPs in varying PEG ratios at pH=7.4. No release was observed because of the neutral pH of the media (Figure 3.16 and Figure 3.17). Thus, acidic media is a requirement for release of the drug from the nanoparticles.

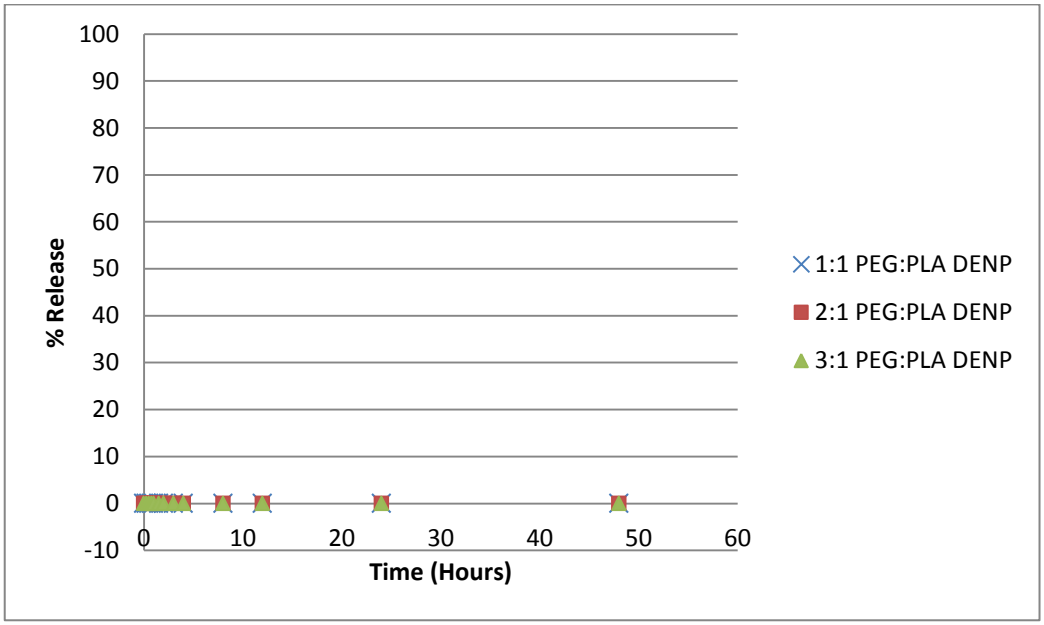

Figure 3.16. Dox (**11**) release from PEG:PLA NPs at pH=7.4.

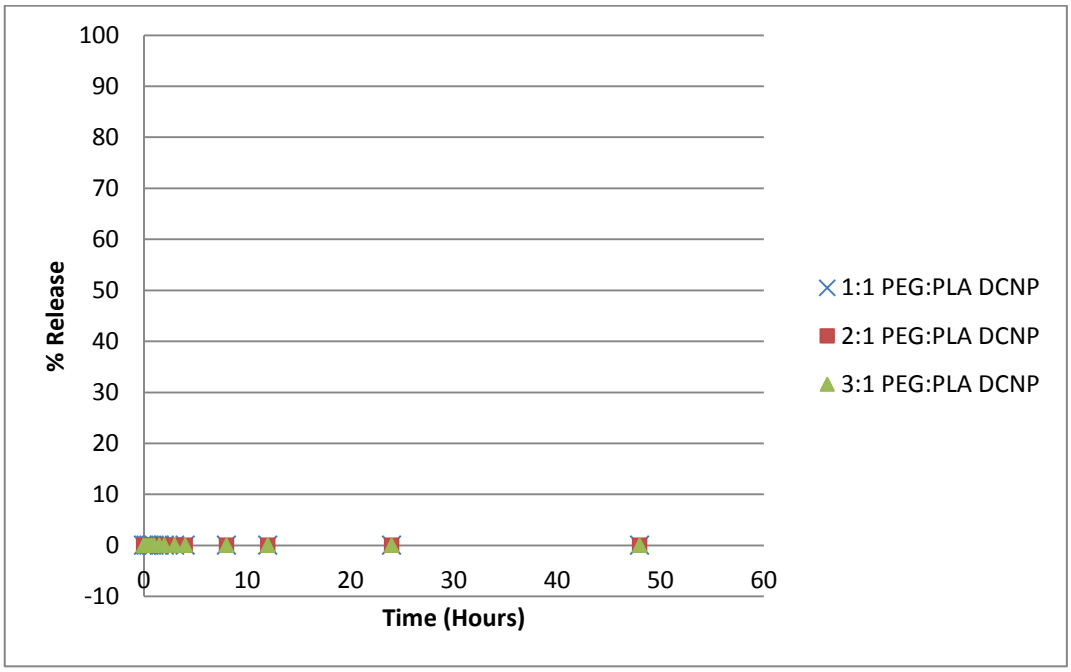

Figure 3.17. Dox-EMCH (**13**) release from PEG:PLA nanoparticles at pH=7.4.

The release behavior of the dox in different batches of NPs which have different contents and ratios of the polymers were examined in pH=5.4. In order to see the effect of PEG contribution, different PEG:PLA ratios by weight were applied. The results can be seen in Figure 3.18. In 0:1 batch, no release of the drug is observed. So the release requires hydrophilic PEG fraction to increase the hydrophilicity of the NP, loosen the highly packed structure of PLA-carbonate copolymer based NPs. As PEG ratio increases, percentage of the amount of released drug increases as expected. At the end of 2 days, sample 1:1 has 9.33±0.42 %, 2:1 has 21.49±1.53 % and 3:1 has 80.44±8.71 % release ratio.

In these initial studies, the drug is not covalently bound to NPs during nanoprecipitation because there is no maleimide linker in hydrophobic dox. Efficient but a rapid release is observed for the 3:1 PEG:PLA formulation while a slower release is observed for constructs with lower amount of PEG polymers.

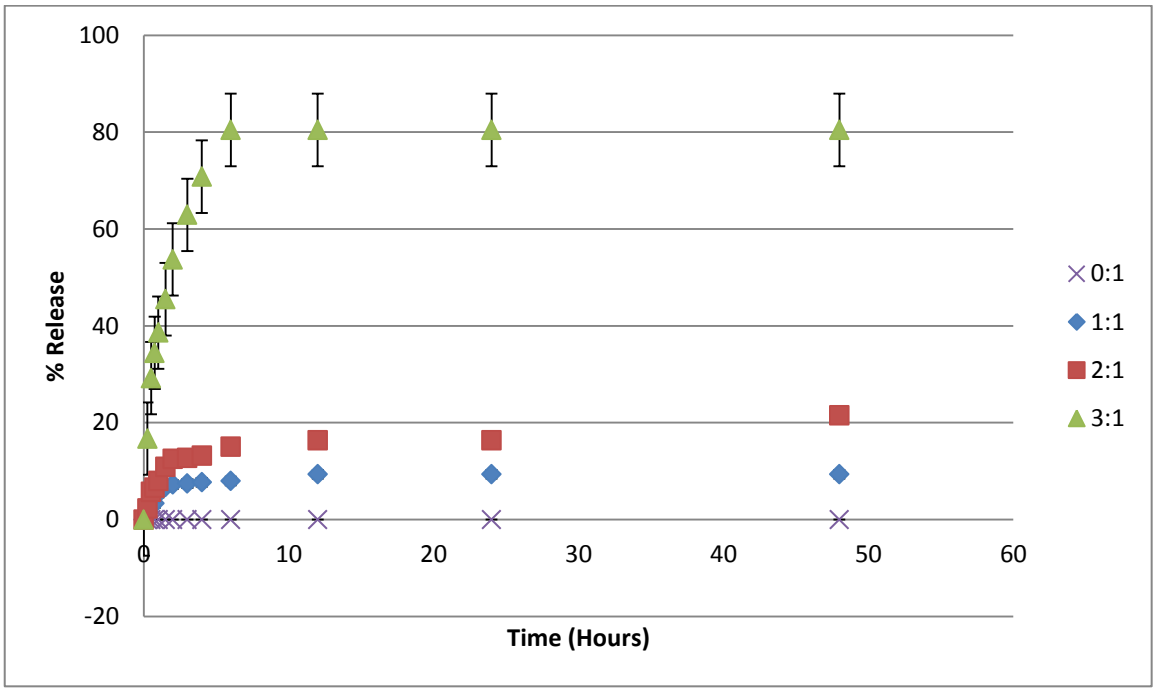

Figure 3.18. Dox (**11**) release from PEG:PLA nanoparticles at pH=5.4.

In the other release study, maleimide-dox (**13**) in used as drug. During the nanoprecipitation, the drug is chemically bound to the furan-bearing PLA-carbonate copolymer via Diels-Alder reaction. So the encapsulation efficiencies are higher than the dox (**11**) encapsulated NPs.

The release profiles of Dox-EMCH (**6**) conjugated NPs can be seen in Figure 3.19. A 0:1 PEG:PLA nanoparticle sample has 0 % release, which means absence of PEG prevented the release of the drug again. Nanoparticle samples with PEG fractions:1:1, 2:1 and 3:1 have 5.35±2.18 %, 36.32±1.72 % and 36.54±1.32 % release respectively at the end of 2 days. As PEG ratio increases, percentage of the amount of released drug increases again as expected.

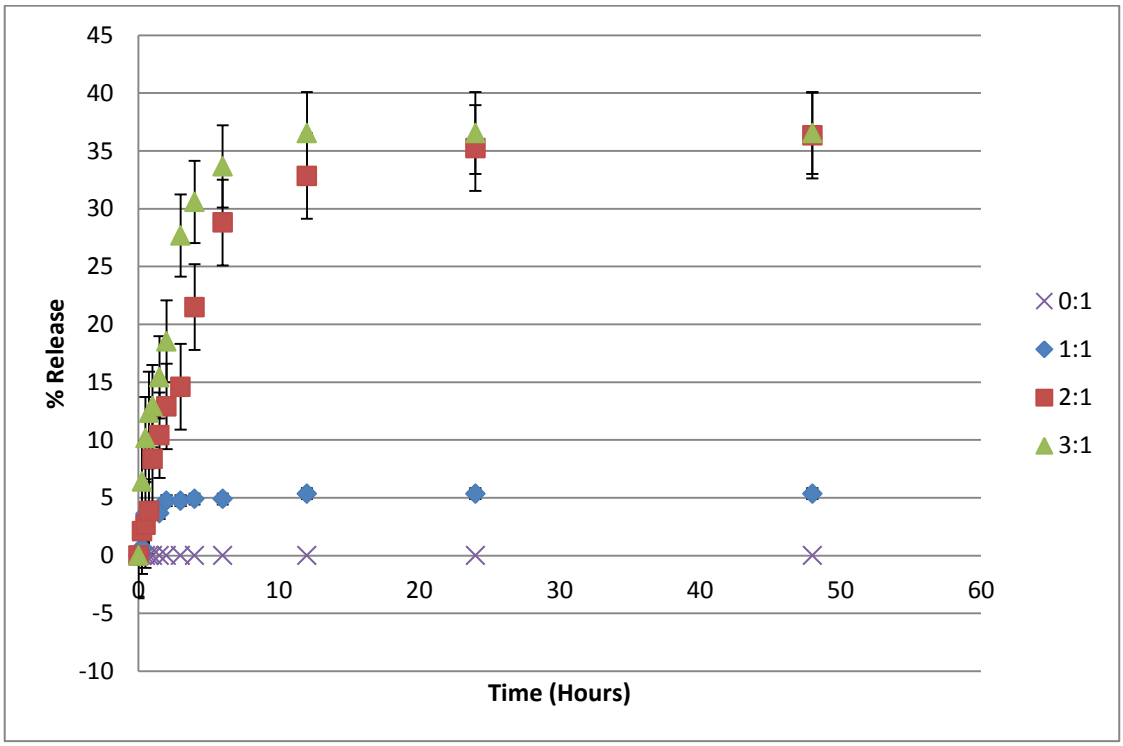

Figure 3.19. Dox-EMCH (**6**) release from PEG:PLA nanoparticles at pH=5.4.

Burst release data (Figure 3.20) clarifies the significant role of conjugation of the drug to the nanoparticles. Presence of hydrazone linkage between the drug and the polymer reduced the burst drug release because it took longer time to be broken under acidic conditions before release compared to diffusion time of non-conjugated drug.

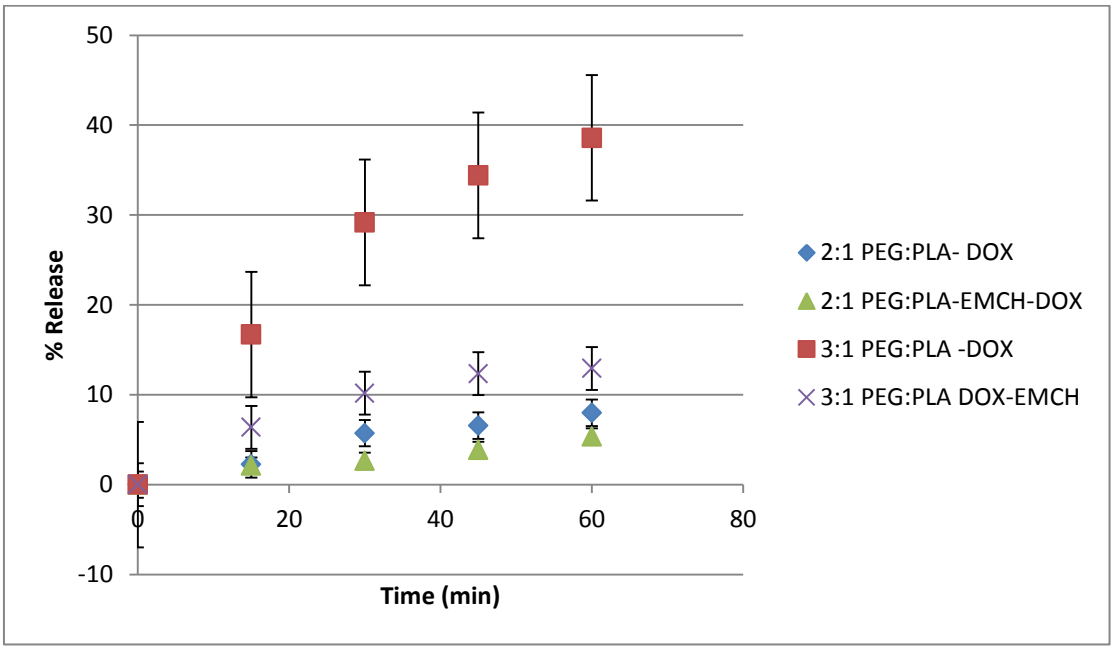

Figure 3.20. Burst release of the drug in the first hour at pH=5.4.

Total release percent values can be seen in Table 3.3. In samples NP 1-3, there were no PEG-conjugation to the NPs. For this reason no release is observed even the drug was conjugated or not. As the PEG ratio increased among NP 4-6, total drug release percent value increased due to the fact that PEG reduced the compactness of the NPs and widened the pores on the surface of the NPs for more passage of the drug. Because of the same reason, drug-conjugated NPs 7-9 indicated the similar results.

Table 3.3. Total release percent values of different NP constructs.

NP #	PEG:PLA	Total Release (%)
NP 1	0:1	0
NP 2	0:1	0
NP 3	0:1	0
NP 4	1:1	9.32 ± 0.42
NP 5	2:1	21.49 ± 1.53
NP 6	3:1	80.44 ± 8.71
NP 7	1:1	5.35 ± 2.18
NP 8	2:1	36.32 ± 1.71
NP 9	3:1	36.54 ± 2.02

3.3. The General Method for Preparation of Third Generation Nanoparticles

3.3.1. cRGDfK-Maleimide Attachment to Nanoparticles for Targeting

For *in vitro* studies, the affinity of the NPs is increased via attachment of cRGDfK linker to NPs using the Diels-Alder reaction. Maleimide-cRGDfK molecule binds to furan groups of the polymer and stays outside of the NP and is able to bind $\alpha_v\beta_3$ integrin receptor of MDA-MB 231 cells. It can be expected that along with this targeting group, NPs will be recognized by the cancer cells with overexpressed receptors and will internalize them efficiently compared to normal healthy cells.

cRGDfK-maleimide was conjugated to second generation nanoparticles via Diels-Alder reaction (Figure 3.21). In NP 10-12 batches preparation (Table 3.4), initially only the polymers and the drug are dissolved in organic solvent and mixed with distilled water drop-wise. After 8 hours, the targeting group is dissolved in very tiny amount of organic solvent and added to NP solution. The reason of addition of targeting group after some time is that the targeting group should bind to the outside of the NPs to easily attach to the receptors found on the cell membrane in cell culture studies.

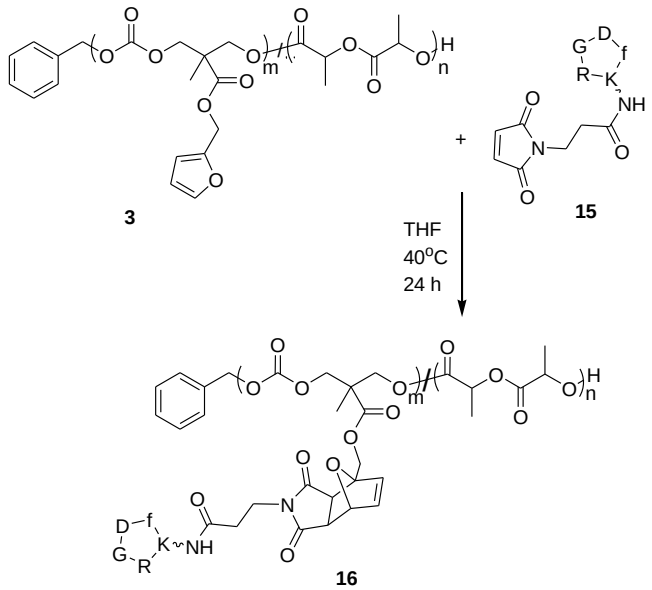

Figure 3.21. Attachment of cRGDfK-maleimide to PLA-carbonate (**3)** copolymer.

Table 3.4. Different combinations of the polymer type, drug type and targeting group in various batches of third generation NPs.

	Drug	Polymer 1	Polymer 2	Targeting Group	DLS Measurement			
NP #	Dox-EMCH	PLA-Furan	PEG-Maleimid	cRGDfK-Maleimid	Size (nm)	PDI	EE (%)	Wt %
10	+	+	+	+	107.7 ± 59.59	0.181	44.5 ± 12.1	1.11
11	+	+	+	+	134.3 ± 103.3	0.408	40.8 ± 6.6	1.02
12	+	+	+	+	112.1 ± 65.4	0.249	23.7 ±4.5	0.59

It is important to ascertain that all unbound targeting peptides are removed from the nanoparticle solution to avoid any competitive binding to the receptors and thus lower the expected enhancement in binding. In order to detect the presence of any residual cRGDfK in the nanoparticle solution even after centrifugation, BCA Protein Assay was applied. In this assay, albumin protein concentration was used as a reference and absorbance values of the supernatants were obtained after each centrifuge with UV-Vis. The absorbance values at 562 nm and their corresponding peptide weight were calculated according to the standard curve obtained with assay kit solutions (Table 3.5). According to this data, only one washing was enough to get rid of all free cRGDfK. NP 10 showed the least amount unbound cRGDfK among three samples because it had the least amount of PEG, and NP 12 had the highest amount of free targeting group because of the highest amount of PEG bound to furan groups of polymer **3** and there was no more free furan groups for that.

Table 3.5. BCA Protein Assay results.

	NP 10		NP 11		NP 12	
Wash #	A562	Weight (μg)	A562	Weight (μg)	A562	Weight (μg)
1	0.017	67.2	0.021	83.1	0.029	90.7
2	0	0	0	0	0	0
3	0	0	0	0	0	0

3.4. *In Vitro* Cytotoxicity

In order to investigate the cytotoxic effect of DCNPs and targeting group-bearing DCNPs, *in vitro* cytotoxicity tests were done. CCK-8 Assay was used to obtain quantitative data. EC_{50} values were calculated according to the absorbance values obtained from using a

microplate reader. These EC_{50} values indicate the drug concentration needed to kill half of the cells. So the lower the EC_{50} values, the more effective is the drug formulation.

In this study MDA-MB 231 breast cancer cell line was used since it is known that the integrin receptors are over-expressed in this type of cancer cells. Drug concentration was varied between 10^{-5} and 10^{-9} M ten-fold. As seen in Figure 3.22, empty NPs have no effect in killing the MDA-MB 231 cells because the building block polymers of the NPs are biocompatible and non-toxic, so in all concentrations of the NPs cell viability is around 100 %. It was observed that while free dox had $EC_{50} = 4.42 \times 10^{-7}$M, and similar values were obtained for the DCNPs ($EC_{50} = 4.25 \times 10^{-7}$ M), the cRGDfK-DCNPs showed an increased ($EC_{50} = 5.19 \times 10^{-8}$ M). $p < 0.001$ for all of the data sets. According to the obtained results, it can be concluded that the incorporation of peptide-based targeting groups increases the effectiveness of the NP delivery vehicle via binding to the integrin receptors found on breast cancer cell membrane which facilitates the internalization of the drug loaded NPs to these cells.

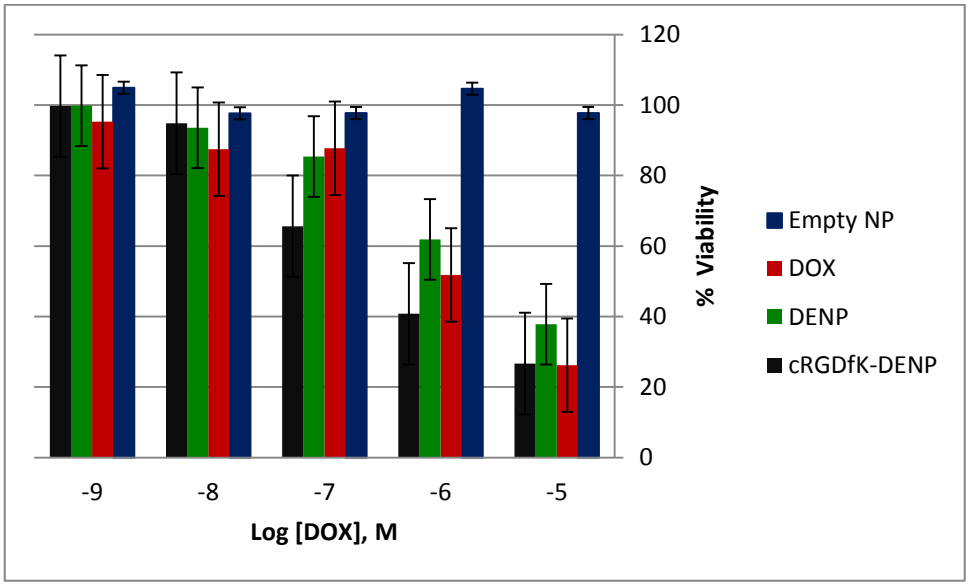

Figure 3.22. Percent viability of MDA-MB 231 cells with different NP or drug constructs.

3.5. Assessment of Drug Internalization by Cells Using Fluorescence Microscopy

In order to show the internalization of the inherently fluorescent drug dox by MDA-MB 231 breast cancer cells, the cells were incubated with different batches of NPs and after 3 h, the images were taken with fluorescence microscopy (Figure 3.23). The aim was to understand the effect of targeting group on DCNPs on internalization and also to understand if there was an effect of different amount of PEG on cellular uptake.

Control samples were incubated with only medium, so it was used to show that the cells were normally healthy and alive. As a positive control, free dox treated cells were studied to show that the drug itself can effectively penetrate to the nuclei of the cells. To ascertain the effect of the targeting group on internalization of the NPs by the cells three types of NPs were utilized. Cells were treated with DCNPs devoid of any targeting units, cRGDfK attached DCNPs and cRGDfK attached NPs along with free cRGDfK. The aim of the last set was to demonstrate that the internalization of the cRGDfK attached DCNPs is indeed due to binding with the integrin receptors. The excess free cRGDfK acts as a competitive inhibitor and reduces the attachment of cRGDfK attached NPs to the integrin proteins on the cell membrane by binding to them and thus blocking them.

During the internalization studies, the cells were also labelled with DAPI to verify the location of the nuclei of the cells because it strongly binds to adenine-thymine rich regions in the DNA. Overlay of red color of dox and blue color of DAPI will indicate localization of the drug in the nucleus.

Free dox applied cells easily uptake this molecule because of its small size. NP 9 (3:1 PEG:PLA DCNP) applied cells internalized more drug than NP 8 (2:1 PEG:PLA DCNP) applied cells because of more PEG attachment made it easy to release the contents of the NPs. Nevertheless, NP 8 and NP 9 solution applied cells showed little internalization because of absence of the targeting group on them. The cells with NP 11 (2:1 PEG:PLA DCNP-cRGDfK) showed much more internalization of dox than the ones without the targeting group even 3 h incubation even more than free drug. The negative control group (2:1 PEG:PLA DCNP-

cRGDfK + free cRGDfK) showed reduced uptake due to simultaneous incubation of free cRGDfK and cRGDfK-bound NPs. Free targeting groups bound to the receptors on the cell membrane before the NPs and prevented NP binding. Therefore, less red color was observed.

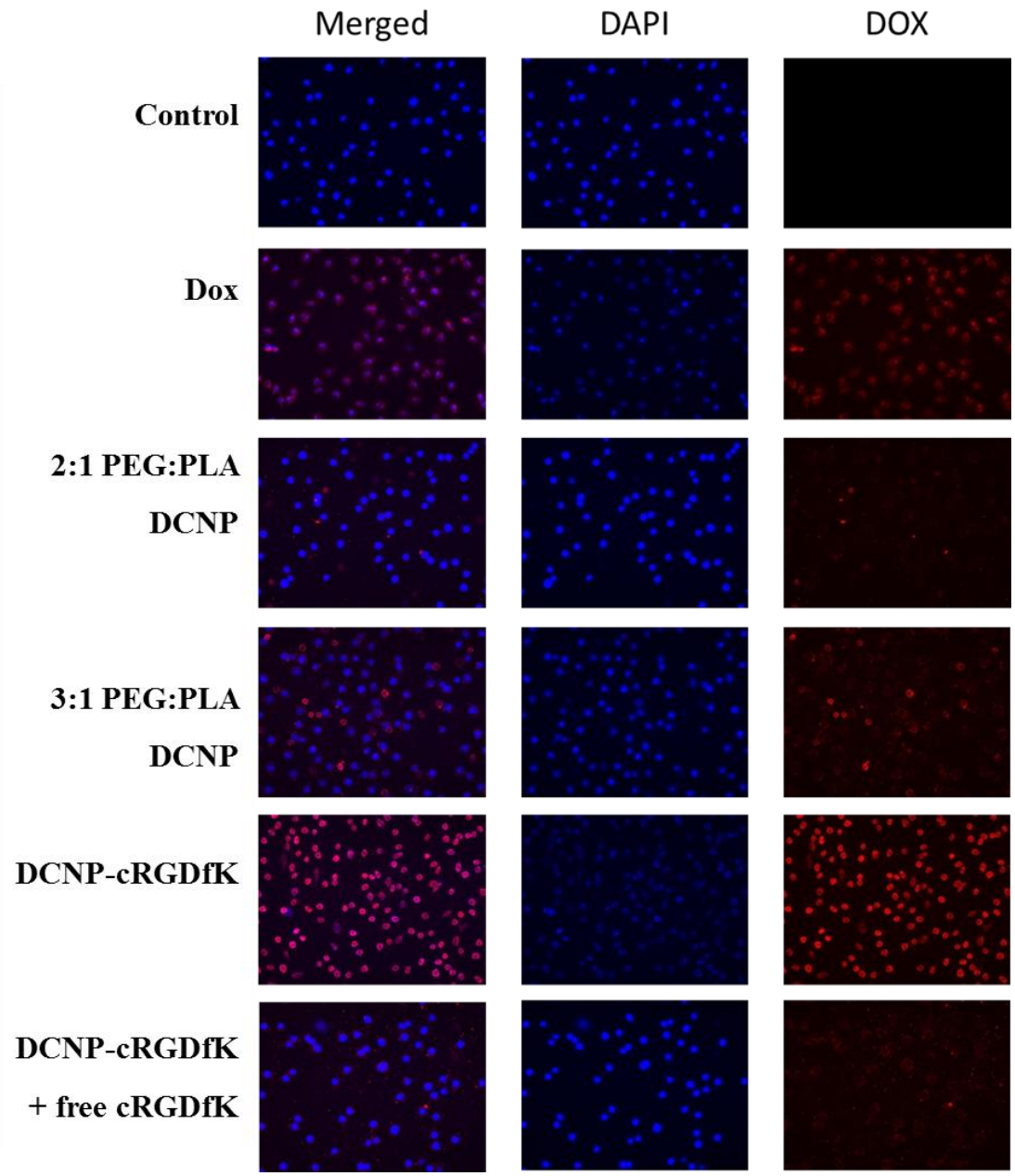

Figure 3.23. Fluorescence microscopy images of different NP samples with the same amount of Dox.

3.6. Detection of Drug Internalization by the Cells with Flow Cytometry

In order to verify the positive effect of the targeting group on cell internalization, the MDA-MB 231 cells are incubated with free Dox, DCNP, cRGDfK-DCNP and mixture of cRGDfK-DCNP and free cRGDfK.

After incubation of the cells with different drug and NP-drug solutions for 3 h, the cells were trypsinized and centrifuged. By this way, free drug, the free polymer and free targeting group which were still in the medium were poured off and therefore flow cytometer detected only the internalized drug fluorescence.

The results seen in Figure 3.24, suggest similar internalization pattern as observed with fluorescence microscopy results. cRGDfK-DCNP treated cells showed the highest intensity of red fluorescence intensity (pink histogram), so the targeting group was highly efficient in internalizing the NPs into the cells. This was followed by free dox treated cells (green histogram). NP 8 (2:1 PEG:PLA DCNP), NP 9 (3:1 PEG:PLA DCNP) and NP 11 (2:1 PEG:PLA DCNP-cRGDfK) + free cRGDfK treated cells (light blue, dark blue and red histograms respectively) indicated similar amounts of drug-internalized cells. The yellow histogram indicated the control group which was incubated with only medium and gave comparatively lower fluorescence.

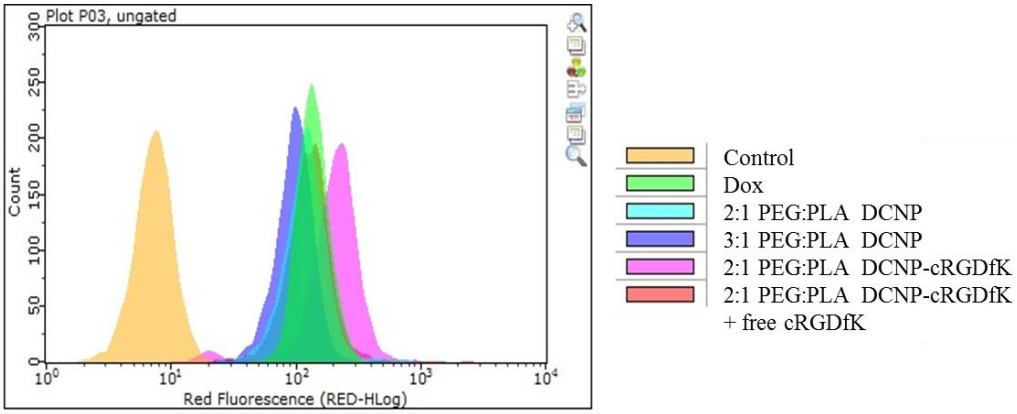

Figure 3.24. Flow cytometry histogram data of different NP samples with the same amount of drug.

4. EXPERIMENTAL

4.1. Synthesis of Furan-Bearing PLA-Carbonate Copolymer

Furan-bearing cyclic carbonate (168 mg,0.7 mmol), benzyl alcohol (1.81 μL, 1.75 x 10^{-2} mmol), L-lactide (400 mg, 2.78 mmol), 1-(3,5-bis(trifluoromethyl)phenyl)-3-cyclohexyl-thiourea (TU) (32.41 mg, 8.75 x 10^{-2} mmol) and 1,8-diazabicycloundec-7-ene (DBU) (13 μL, 8.75 x 10^{-2} mmol) were placed in a vial under nitrogen atmosphere in a glove box and left to stir for 20 h at room temperature in dry CH_2Cl_2 (3 mL). The resulting polymer (**3**) was purified by precipitation from 1:1 methanol:diethyl ether mixture (conversion = 65%). According to GPC, M_n = 12 363 Da, M_w = 14 713 Da, M_w/M_n = 1.19. PDI = 1.3. ^{1}H NMR ($CDCl_3$, δ, ppm) 7.29 (s, 1H, −CH═), 7.25 (s, 5H, −CH═), 6.38 (s, 1H, −CH═), 6.33 (s, 1H,−CH═), 4.25 (m, 4H, CH_2CO), 1.50-1.64 (m, 6H, −CH_3), 1.22 (s, 3H, −CH_3).

4.2. Synthesis of Mono-Maleimide PEG

To a solution of dried polyethylene glycol monomethylether 750 (PEG) (1.50 g, 2 mmol) dissolved in THF (6 mL), triethylamine (0.42 mL, 3.00 mmol) was added at 0 °C. In a separate flask, succinic anhydride (0.3 g, 3.00 mmol) and DMAP (0.048 g, 0.40 mmol) were dissolved in THF (6 mL) and transferred drop wise onto the PEG solution at 0 °C for more than 30 min. The clear solution was stirred for 20 h at room temperature under N_2. The crude was concentrated and purified with column chromatography. The product was dried under vacuum, to give pure mono-acid PEG as white solid (0.8 g, 44,4% yield). Then, mono-acid PEG (0.75 g, 1.00 mmol) was dried under vacuum after azeotropic distillation with toluene. Mono-acid PEG dissolved in CH_2Cl_2 (5 mL), the furan-protected maleimide group containing alcohol (0.687 g, 3.00 mmol), DMAP (0.12 g, 0.10 mmol), and EDCI (0.21 g, 1.10 mmol) were added. The solution was stirred for 20 h at room temperature under N_2. To the reaction mixture, CH_2Cl_2 (20 mL) was added and the mixture was washed with saturated $NaHCO_3$ (2 × 15 mL). The combined organic layers were dried over anhydrous Na_2SO_4 and all volatiles were evaporated. The crude was purified via column chromatography and pure furan protected mono-maleimide PEG was dried under vacuum as a pink solid (0.7 g, 87.5 % yield). Furan protected mono-maleimide PEG is spread into 100 ml round bottom flask and retro Diels-

Alder is applied to it to obtain mono-maleimide PEG (**9**) under vacuum for 3 hours at 111°C (0.6 g, 85.7 % yield). The product is checked with ^{1}HNMR.

^{1}H NMR ($CDCl_3$, δ, ppm), 6.71 (s, 2H,–CH═) , 4.22 (t, 2H, J = 4.8 Hz, OCH_2), 4.03 (t, 2H, J = 6.4 Hz, NCH_2), 3.82–3.41 (m, 4H, OCH_2CH_2 of PEG), 3.35 (s, 3H, OCH_3 of PEG), 2.69–2.60 (m, 4H, CH_2C═O), 1.89 (tt, 2H, J = 6.0, 4.8 Hz, $NCH_2CH_2CH_2O$).

4.3. Synthesis of Maleimide-Doxorubicin

Dox (12.0 mg, 1.21 x 10^{-2} mmol) and N-ε-maleimidocaproic acid hydrazide (EMCH) linker (14.9 mg, 6.63 x 10^{-2} mmol) were dissolved in methanol (6 mL) and was added trifluoroacetic acid (20 mL). The reaction was stirred under N_2 for 24 h. The solvent was concentrated under *vacuo* until 1 mL was left and this solution was dropped into cold ethyl acetate (10 mL) and kept for 16 h at -20 ^{o}C to precipitate. Then, it was centrifuged for 10 min at 7000 rpm. The supernatant was decanted and again cold ethyl acetate (10 mL) was added. This precipitation procedure was repeated for three times. The resultant precipitate was dried to yield 6 mg (22 % yield) of EMCH-DOX (**13**). The product was characterized via FT-IR.

4.4. Preparation of Nanoparticles

Table 4.1 The masses of the additives in different batches of NPs (mg).

	Drug			Polymer 1		Polymer 2	Targeting Group
NP #	Dox.HCl	Dox	Dox-EMCH	PLA	PLA-Furan	PEG-Maleimid	cRGDfK-Maleimid
1	0.5			10			
2		0.5		10			
3			0.5		10		
4		0.5			10	10	
5		0.5			10	20	
6		0.5			10	30	
7			0.5		10	10	
8			0.5		10	20	
9			0.5		10	30	
10			0.5		10	10	0.1
11			0.5		10	20	0.1
12			0.5		10	30	0.1

Different combinations of Dox, PLA and PEG molecules were dissolved in THF (1 mL) and added onto distilled water (10 mL) drop-wise. The mixture was left to evaporate the solvent at 40 ^{o}C and stirred at 300 rpm for 18 h. Size and PDI measurements were done with DLS. The nanoparticle solution was taken into a 15 mL falcon and centrifuged at 7000 rpm for 10 min to precipitate the nanoparticles. The supernatant contained the drug molecules which were not encapsulated and polymers which did not attend the nanoparticle formation. This supernatant was poured off and the precipitate was re-suspended in distilled water and sonicated for 1 min. Size and PDI measurements were done with DLS to control whether there was still aggregation of nanoparticles after centrifugation.

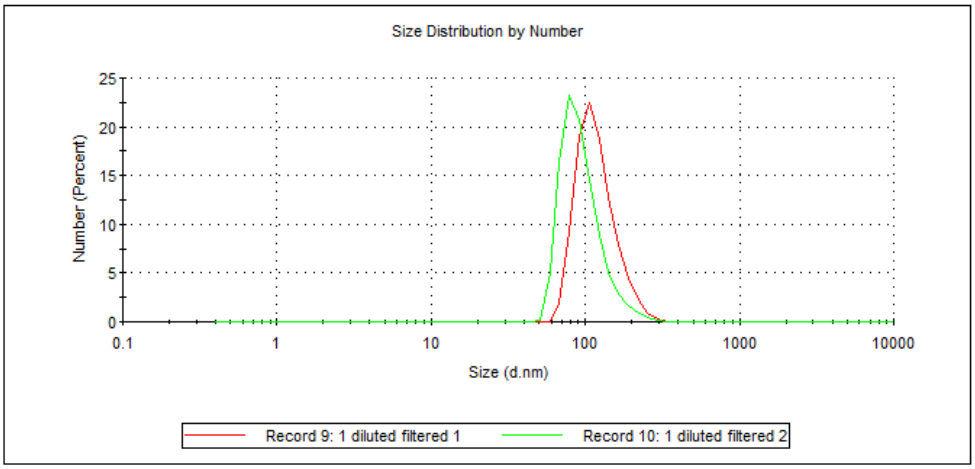

Figure 4.1. DLS result of NP 4.

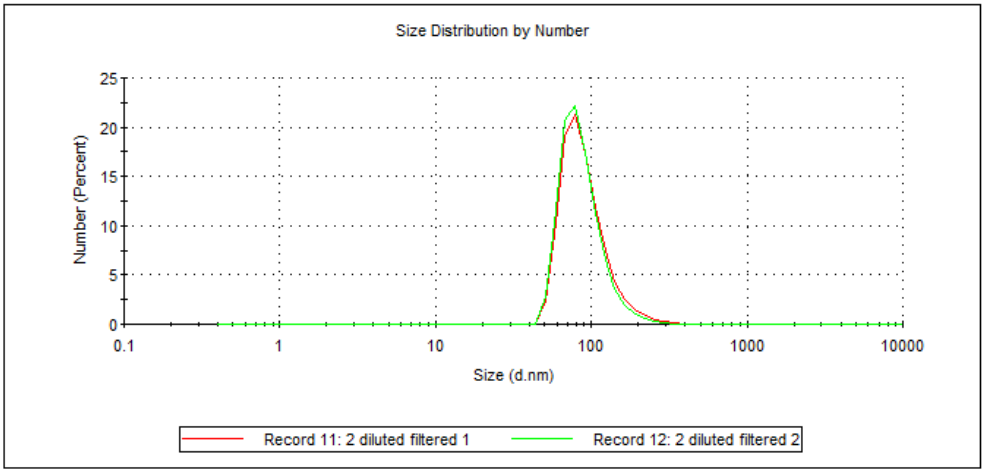

Figure 4.2. DLS result of NP 5.

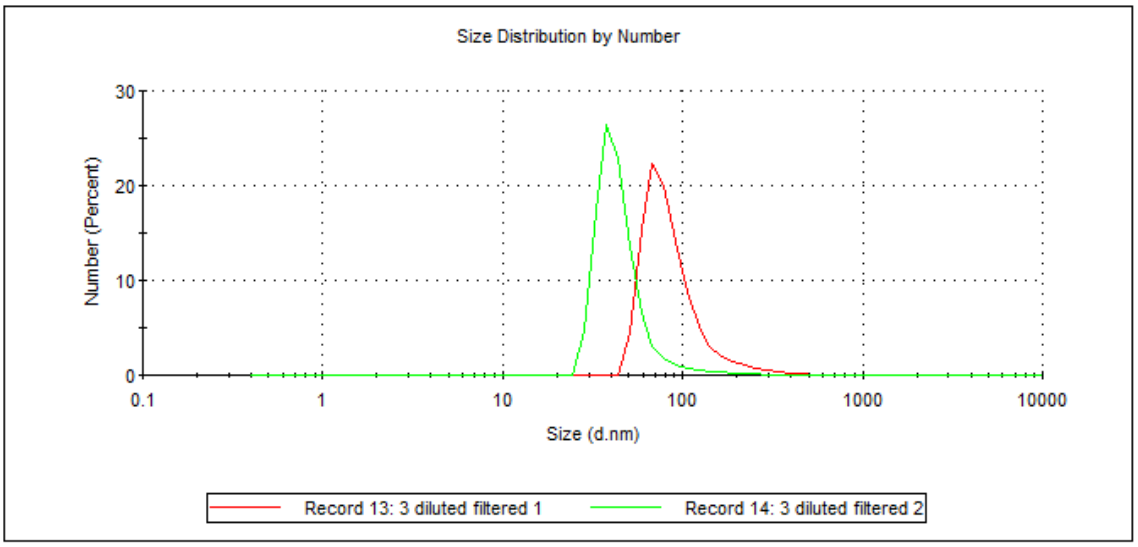

Figure 4.3. DLS result of NP 6.

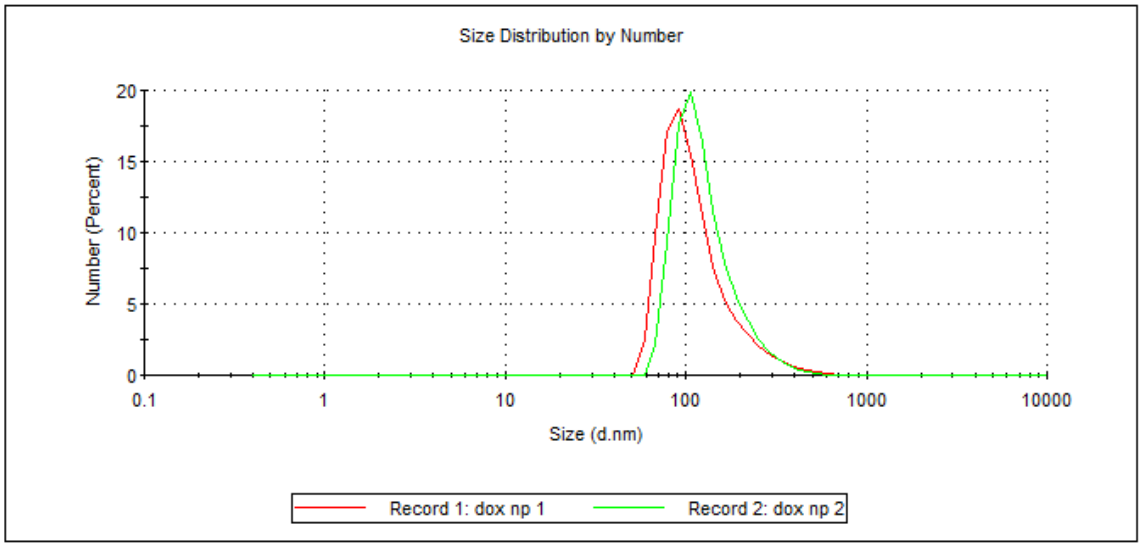

Figure 4.4. DLS result of NP 7.

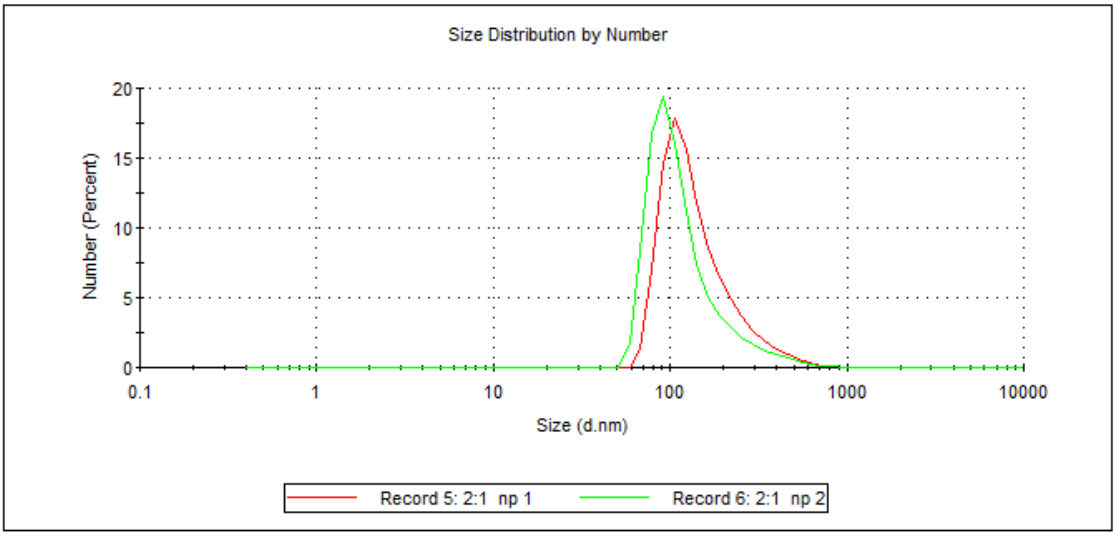

Figure 4.5. DLS result of NP 8.

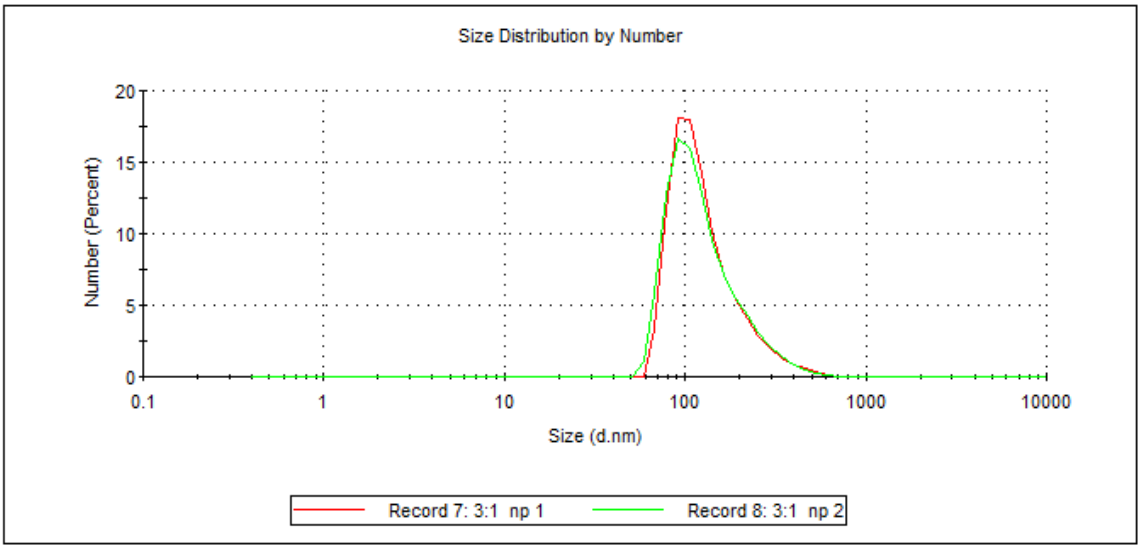

Figure 4.6. DLS result of NP 9.

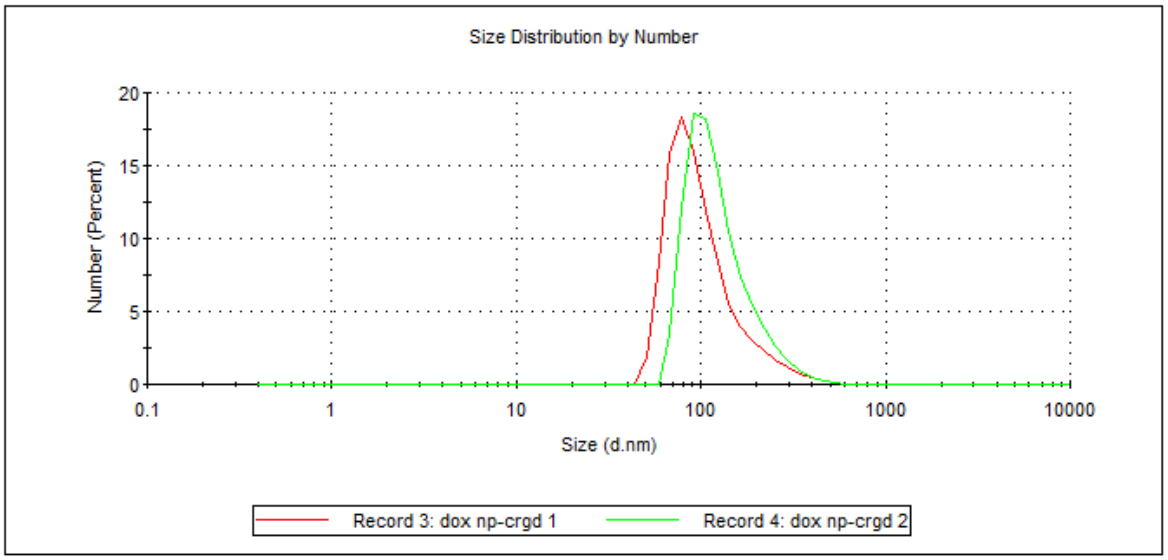

Figure 4.7. DLS result of NP 10.

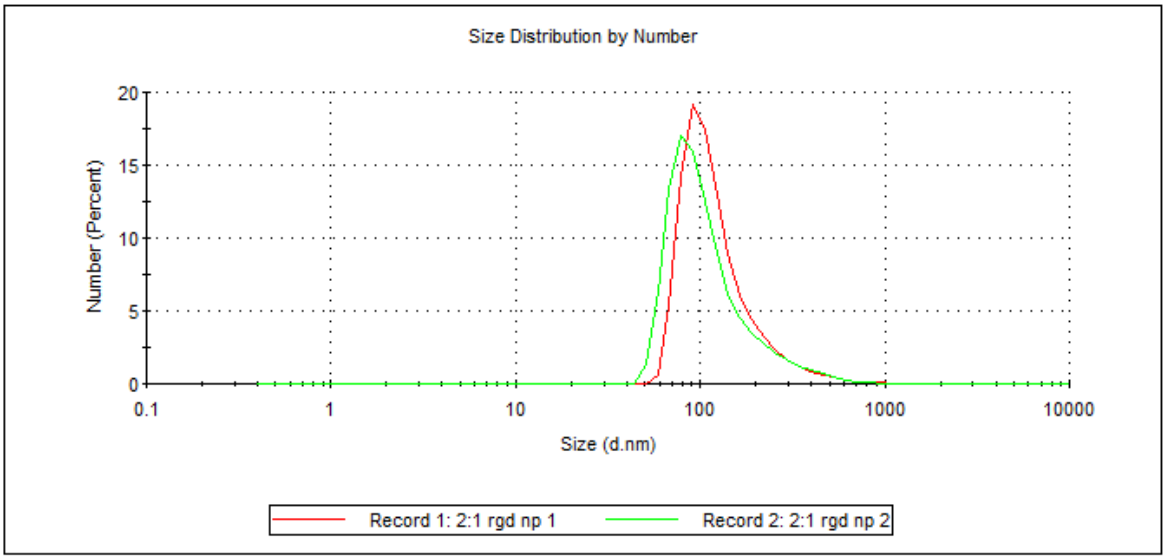

Figure 4.8. DLS result of NP 11.

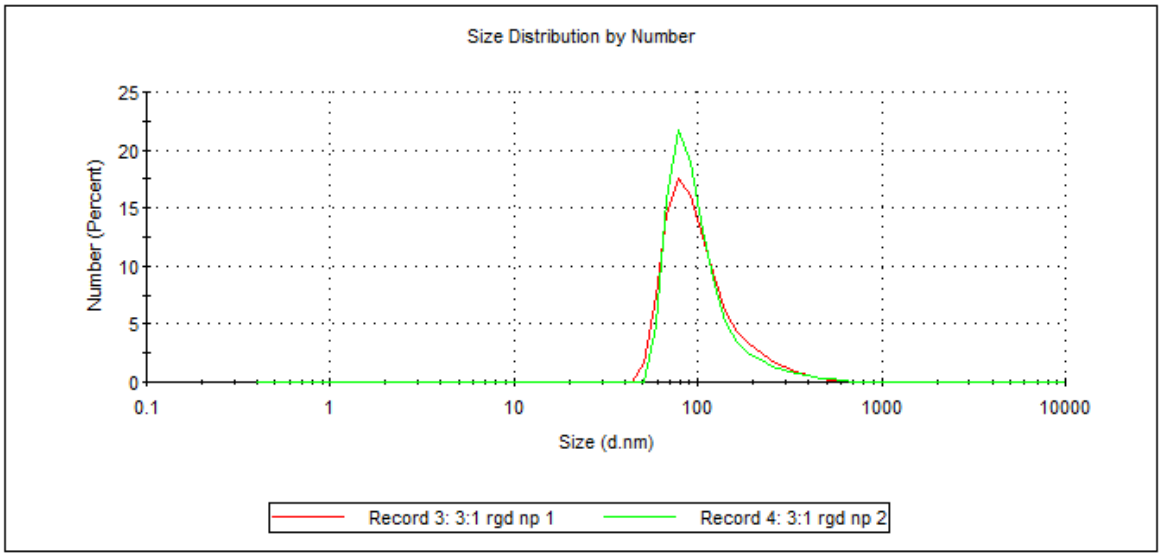

Figure 4.9. DLS result of NP 12.

Table 4.2. DLS results, encapsulation efficiencies (EE) and weight percent of all of the NP batches.

	DLS Measurement			
NP #	Size	PDI	EE (%)	Wt %
4	120.3 ± 36.33	0.034	34.8 ± 6.8	0.87
5	92.29 ± 35.31	0.153	30.7 ± 2.4	0.77
6	90.93 ± 49.41	0.260	20.1 ± 5.7	0.50
7	120.1 ± 64.58	0.187	70.8 ± 11.2	1.77
8	153.1 ± 92.6	0.270	64.4 ± 8.7	1.61
9	136.4 ± 72.93	0.186	41.0 ± 9.7	1.02
10	107.7 ± 59.59	0.181	44.5 ± 12.1	1.11
11	134.3 ± 103.3	0.408	40.8 ± 6.6	1.02
12	112.1 ± 65.4	0.249	23.7 ±4.5	0.59

4.5. Release of the Drug from the Nanoparticles

1000 MWCO membrane was cut in 10 cm length and washed with citrate buffer (pH=5.4) several times. The bottom of the membrane was tied with a copper wire and filled with the nanoparticle solution. The upper part of the membrane was also tied with a copper

wire and it was placed in a 50 mL falcon which contained citrate buffer (pH = 5.4) (10 mL). The falcon containing the release setup was placed at 37 ^{o}C and stirred at 150 rpm. At every time point, a sample (1 mL) was taken from out of the membrane and the solution was completed to 10 mL with fresh citrate buffer again. Citrate buffer (1 mL) was added onto the taken sample. The drug amount in the samples was obtained with Fluorescent Spectroscopy and its absorbance values were used in calculation according to the calibration curve.

4.6. *In Vitro* Cytotoxicity

MDA-MB 231 human breast cancer cell line was used for cytotoxicity experiments. RPMI medium was used to grow the cells. The edge row and column wells of a 96-well plate were filled with distilled water (100 µL/well). The cells were seeded in rest of the wells in 5,000 cell/well density having medium (100 µL/well). After incubation for one day, between 10^{-5}-10^{-10}M of drug containing nanoparticle solutions (in medium) were given to the cells (100 µL/well). After 48 h of drug incubation CCK-8 Assay was applied. For this assay, 10 % CCK-8 solution containing medium (60 µL/well) was applied and incubated for 2 h. The absorbance measurements were taken with MultiScan. According to these absorbance values, IC_{50} values of different batches of the nanoparticles were calculated with GraphPad Prism.

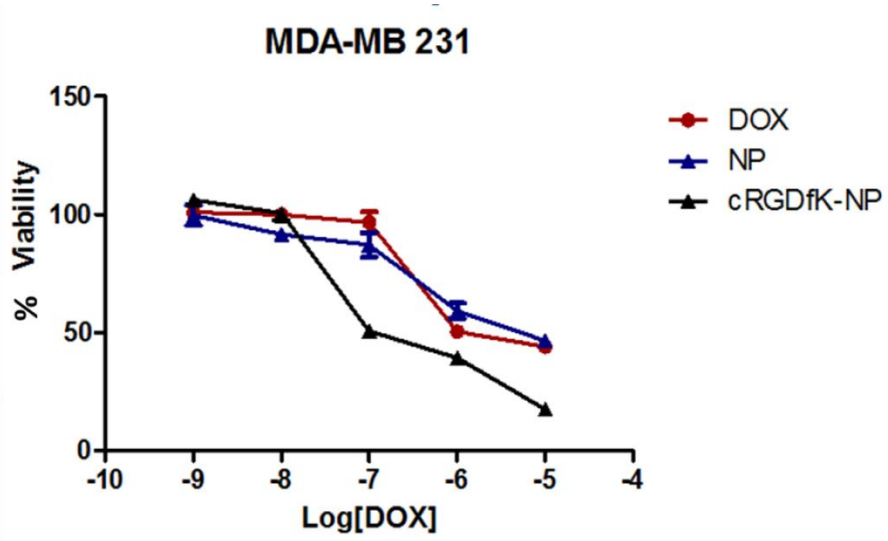

Figure 4.10. Percent viability of MDA-MB 231 cells with changing drug concentration.

4.7. Detection of Drug Internalization by the Cells with Flow Cytometer

For flow cytometry experiment, MDA-MB 231 (passage 55) human breast cancer cell line was used. 50,000 cell/well were seeded in 6-well plates. The cells were incubated with 0.5 mg/ml Dox containing nanoparticle solutions and 0.5 mg/ml Dox solutions. After 3 h, the drug containing mediums were removed and the cells were trypsinized with 0.05 % trypsin solution. After neutralizing trypsin with medium, cells were centrifuged at 300 rpm for 5 min. After that the cells were re-suspended in 1X PBS solution and given to flow cytometry.

4.8. Cell Imaging with Fluorescence Microscope

For imaging the cells with fluorescence microscopy, MDA-MB 231 (passage 55) human breast cancer cell line was used. 50,000 cell/well were seeded in 6-well plate. The cells were incubated with dox (0.5 mg/ml) containing nanoparticle solutions and dox (0.5 mg/ml) solutions. After 3 h, the dox containing mediums were removed and DAPI solutions in 1 X PBS were applied for 30 min. After DAPI incubation, the solutions were removed and the cells were washed with 1 X PBS 3 times. Then red and blue filters were used to obtain fluorescence microscopy images.

5. CONCLUSION

In this study, two generations of PLA-based drug encapsulated polymeric nanoparticles were formulated using nanoprecipitation and their drug encapsulation, drug release and cellular targeting efficiencies were evaluated. The first generation polymeric nanoparticles were prepared by using PLA as a building block. Dox was loaded into nanoparticles physically. In order to increase the encapsulation efficiency of the nanoparticles, maleimide-attached-drug was conjugated to the furan-bearing PLA-carbonate copolymer which was synthesized via ring-opening polymerization. In release studies of these nanoparticles, poor results were obtained. It was hypothesized that the highly hydrophobic nature of the construct was responsible for lack of drug release.

To address this issue, second generation of PLA-nanoparticles with enhanced hydrophilicity were formulated. For this, a polyethylene glycol (PEG) containing fragment (maleimide-PEG) that can be attached to the nanoparticle, was synthesized and conjugated to the copolymer to produce second generation nanoparticles. The attachment of the PEG fractions resulted in a drastic increase in the release of the drug. Furthermore, a slower initial release was witnessed when the drug was covalently attached to the nanoparticles.

Maleimide-cRGDfK was attached to the second generation nanoparticles as targeting group to evaluate cellular targeting through *in vitro* studies to generate third generation nanoparticles. *In vitro* studies revealed that the empty nanoparticles were non-toxic and drug loaded nanoparticles were efficiently internalized by MDA-MB-231 cells. Furthermore, both flow cytometry and fluorescence microscopy analysis revealed enhanced uptake of drug loaded nanoparticles decorated with peptide based targeting group.

APPENDIX A: SPECTROSCOPY DATA

^{1}HNMR data for a synthesized compound is given.

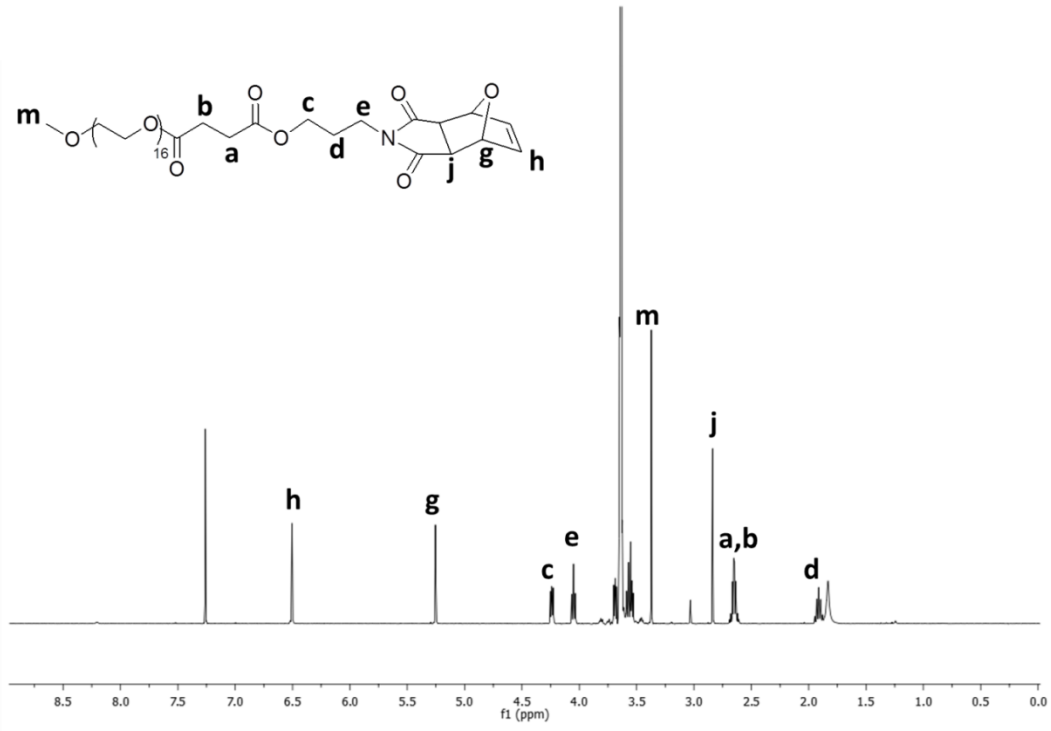

Figure A.1. ^{1}HNMR spectra of Furan-Protected Maleimide Group Bearing Monomethoxy PEG.

REFERENCES

1. http://globocan.iarc.fr/Pages/fact_sheets_cancer.aspx [Accessed on February 2015].

2. Chaffer, C. L., and R. A. Weinberg, "A Perspective On Cancer Cell Metastasis." *Science (New York, N.Y.)*, Vol. 331, pp. 1559–64, 2011.

3. Swift, L. P., A. Rephaeli, A. Nudelman, D. R. Phillips, and S. M. Cutts, "Doxorubicin-DNA Adducts Induce A Non-topoisomerase II-mediated Form Of Cell Death." *Cancer Research*, Vol. 66, pp. 4863–4871, 2006.

4. Lung cancer guide book, "Chemotherapy Side Effects Profile." *Lung Cancer Guide Book*, pp. 384–395, 2013.

5. Friberg, L. E., and M. O. Karlsson, "Mechanistic Models For Myelosuppression." *Investigational New Drugs*, Vol. 21, pp. 183–194, 2003.

6. Yamashita, F., and M. Hashida, "Pharmacokinetic Considerations For Targeted Drug Delivery." *Advanced Drug Delivery Reviews*, Vol. 65, pp. 139–47, 2013.

7. Bazak, R., M. Houri, S. El Achy, W. Hussein, and T. Refaat, "Passive Targeting Of Nanoparticles To Cancer: A Comprehensive Review Of The Literature." *Molecular and Clinical Oncology*, Vol. 2, pp. 904–908, 2014.

8. Maeda, H., K. Greish, and J. Fang, "The EPR Effect And Polymeric Drugs: A Paradigm Shift For Cancer Chemotherapy In The 21st Century." *Advances in Polymer Science*, Vol. 193, pp. 103–121, 2006.

9. Torchilin, V., "Tumor Delivery Of Macromolecular Drugs Based On The EPR Effect." *Advanced Drug Delivery Reviews*, Vol. 63, pp. 131–135, 2011.

10. Marelli, U. K., F. Rechenmacher, T. R. A. Sobahi, C. Mas-Moruno, and H. Kessler, "Tumor Targeting Via Integrin Ligands." *Frontiers in Oncology*, Vol. 3, pp. 222, 2013.

11. Danhier, F., O. Feron, and V. Préat, "To Exploit The Tumor Microenvironment: Passive And Active Tumor Targeting Of Nanocarriers For Anti-cancer Drug Delivery." *Journal of Controlled Release*, Vol. 148, pp. 135–46, 2010.

12. Byrne, J. D., T. Betancourt, and L. Brannon-Peppas, "Active Targeting Schemes For Nanoparticle Systems In Cancer Therapeutics." *Advanced Drug Delivery Reviews*, Vol. 60, pp. 1615–26, 2008.

13. Ang, C. Y., S. Y. Tan, and Y. Zhao, "Recent Advances In Biocompatible Nanocarriers For Delivery Of Chemotherapeutic Cargoes Towards Cancer Therapy." *Organic & Biomolecular Chemistry*, Vol. 12, pp. 4776–806, 2014.

14. Siegel, R. A., and M. J. Rathbone, "Overview Of Controlled Release Mechanisms." *Fundamentals and Applications of Controlled Release*, pp. 19–44, 2012.

15. Lee, E., "Polymeric Micelle For Tumor PH And Folate-mediated Targeting." *Journal of Controlled Release*, Vol. 91, pp. 103–113, 2003.

16. Lee, S. J., H. Koo, H. Jeong, M.S. Huh, Y. Choi, S. Y. Jeong, Y. Byun, K. Choi, K. Kim, and I. C. Kwon, "Comparative Study Of Photosensitizer Loaded And Conjugated Glycol Chitosan Nanoparticles For Cancer Therapy." *Journal of Controlled Release*, Vol. 152, pp. 21–29, 2011.

17. Chen, J., J. Ouyang, J. Kong, W. Zhong, and M. M. Xing, "Photo-cross-linked And PH-sensitive Biodegradable Micelles For Doxorubicin Delivery." *ACS Applied Materials and Interfaces*, Vol. 5, pp. 3108–3117, 2013.

18. Wang, F., Y. Li, Y. Shen, A. Wang, S. Wang, and T. Xie, "The Functions And Applications Of RGD In Tumor Therapy And Tissue Engineering." *International Journal of Molecular Sciences*, Vol. 14, pp. 13447–62, 2013.

19. Liu, S., "Radiolabeled Cyclic RGD Peptides As Integrin Alpha(v)beta(3)-targeted Radiotracers: Maximizing Binding Affinity Via Bivalency." *Bioconjugate Chemistry*, Vol. 20, pp. 2199–213, 2009.

20. Shi, M., K. Ho, A. Keating, and M. S. Shoichet, "Doxorubicin-Conjugated Immuno-Nanoparticles For Intracellular Anticancer Drug Delivery." *Advanced Functional Materials*, Vol. 19, pp. 1689–1696, 2009.

21. Hirsjärvi, S., C. Belloche, F. Hindré, E. Garcion, and J. P. Benoit, "Tumour Targeting Of Lipid Nanocapsules Grafted With CRGD Peptides." *European Journal of Pharmaceutics and Biopharmaceutics*, Vol. 87, pp. 152–159, 2014.

22. Murphy, E. A., B. K. Majeti, L. A. Barnes, M. Makale, S. M. Weis, K. Lutu-Fuga, W. Wrasidlo, and D. A. Cheresh, "Nanoparticle-mediated Drug Delivery To Tumor Vasculature Suppresses Metastasis." *Proceedings of the National Academy of Sciences of the United States of America*, Vol. 105, pp. 9343–9348, 2008.

23. Hossain Saad, M. Z., R. Jahan, and U. Bagul, "Nanopharmaceuticals: A New Perspective Of Drug Delivery System." *Asian Journal of Biomedical and Pharmaceutical Sciences*, Vol. 2, pp. 11–20, 2012.

24. Nasongkla, N., X. Shuai, H. Ai, B. D. Weinberg, J. Pink, D. A. Boothman, and J. Gao, "CRGD-functionalized Polymer Micelles For Targeted Doxorubicin Delivery." *Angewandte Chemie - International Edition*, Vol. 43, pp. 6323–6327, 2004.

25. Pridgen, E. M., R. Langer, and O. C. Farokhzad, "Biodegradable, Polymeric Nanoparticle Delivery Systems For Cancer Therapy." *Nanomedicine,* Vol. 2, pp. 669–680, 2007.

26. Yu, Y., C. K. Chen, W. C. Law, E. Weinheimer, S. Sengupta, P.N. Prasad, and C. Cheng, "Polylactide-graft-Doxorubicin Nanoparticles With Precisely Controlled Drug Loading For PH-Triggered Drug Delivery." *Biomacromolecules,* 2014.

27. Rao, J. P., and K. E. Geckeler, "Polymer Nanoparticles: Preparation Techniques And Size-control Parameters." *Progress in Polymer Science*, Vol. 36, pp. 887–913, 2011.

28. Pinto Reis, C., R. J. Neufeld, A.J. Ribeiro, and F. Veiga, "Nanoencapsulation I. Methods For Preparation Of Drug-Loaded Polymeric Nanoparticles." *Nanomedicine : Nanotechnology, Biology, and Medicine*, Vol. 2, pp. 8–21, 2006.

29. Soppimath, K. S., T. M. Aminabhavi, A. R. Kulkarni, and W.E. Rudzinski, "Biodegradable Polymeric Nanoparticles As Drug Delivery Devices." *Journal of Controlled Release,* Vol. 70, pp. 1–20, 2001.

30. Yang, X., J. J. Grailer, I. J. Rowland, A. Javadi, S. A. Hurley, V. Z. Matson, D. A. Steeber, and S. Gong, "Multifunctional Stable And PH-Responsive Polymer Vesicles Formed By Heterofunctional Triblock Copolymer For Targeted Anticancer Drug Delivery And Ultrasensitive MR Imaging." *ACS Nano*, Vol. 4, pp. 6805–17, 2010.

31. Albertsson, A. C., and I. K. Varma, "Recent Developments In Ring Opening Polymerization Of Lactones For Biomedical Applications." *Biomacromolecules*, Vol. 4, pp. 1466–86, 2003.

32. Dispinar, T., R. Sanyal, and A. Sanyal, "A Diels-Alder/Retro Diels-Alder Strategy To Synthesize Polymers Bearing Maleimide Side Chains." *Journal of Polymer Science*, pp. 4545–4551, 2007.

33. Engel, T., and G. Kickelbick, "Thermoreversible Reactions On Inorganic Nanoparticle Surfaces: Diels-Alder Reactions On Sterically Crowded Surfaces." *Chemistry of Materials*, Vol. 25, pp. 149–157, 2013.

34. Shi, M., J. H. Wosnick, K. Ho, A. Keating, and M.S. Shoichet, "Immuno-polymeric Nanoparticles By Diels-Alder Chemistry." *Angewandte Chemie (International ed. in English)*, Vol. 46, pp. 6126–31, 2007.

35. Tobío, M., A. Sánchez, A. Vila, I. Soriano, C. Evora, J. Vila-Jato, and M.. Alonso, "The Role Of PEG On The Stability In Digestive Fluids And In Vivo Fate Of PEG-PLA Nanoparticles Following Oral Administration." *Colloids and Surfaces B: Biointerfaces*, Vol. 18, pp. 315–323, 2000.

36. Schubert, S., J. T. Delaney and U. S. Schubert, "Nanoprecipitation And Nanoformulation Of Polymers: From History To Powerful Possibilities Beyond Poly(lactic Acid)." *Soft Matter*, Vol. 7, pp. 1581, 2011.